Genetic and Morphological Studies on Goniurosaurus kuroiwae (Squamata: Eublepharidae), with a Description of a New Species from the Northern Part of Okinawajima Island, Ryukyu Archipelago, Japan

Authors: Kurita, Takaki, and Toda, Mamoru

Source: Current Herpetology, 43(1) : 86-114

Published By: The Herpetological Society of Japan

URL: https://doi.org/10.5358/hsj.43.86

Current Herpetology 43(1): 86–114, February 2024 doi 10.5358/hsj.43.86

Genetic and Morphological Studies on *Goniurosaurus kuroiwae* (Squamata: Eublepharidae), with a Description of a New Species from the Northern Part of Okinawajima Island, Ryukyu Archipelago, Japan

Takaki KURITA[1,*] and Mamoru TODA[2]

[1]*Natural History Museum and Institute Chiba, Aoba-cho 955–2, Chuo, Chiba 260–8682, JAPAN*
[2]*Tropical Biosphere Research Center, University of the Ryukyus, Senbaru, Nishihara, Okinawa 903–0213, JAPAN*

Zoobank LSID: 2049918F-E3E2-481F-AB42-D5B3497B9E8F

Abstract: *Goniurosaurus k. kuroiwae* consists of two genetically diverged entities (i.e., northern and southern lineages) that are geographically separated by a narrow hybrid zone in the north–central part of Okinawajima Island, Ryukyu Archipelago, Japan. Our molecular analyses using single nucleotide polymorphism data confirmed their remarkable genetic differentiation. Morphological comparisons using random forest models further revealed that these two lineages could be distinguished by combinations of several characteristics. Considering that these two entities have persisted within a single island, they deserve to be given full species status. The type locality of the nominal species, *G. kuroiwae*, fell within the range of the "southern species" and the morphological features of the holotype agreed well with the "southern species". Hence we described the populations of the northern part of Okinawajima and Kourijima as a new species, *Goniurosaurus nebulozonatus* sp. nov. This new species differs from other congeners in the Ryukyus with a combination of the following character states: reddish brown iris, 4–7 postmentals, flat and imbricate ventral scales, denser tubercles on the femur, single most-enlarged scale on the pes base, mid-dorsal stripe present at the nape and absent in the posterior part of the trunk, incomplete or no nuchal loop, dorsal band on the posterior trunk present, and obscure dorsal stripes/bands. The new species was inferred to be a sister taxon of *G. kuroiwae* sensu stricto, so allocating other taxa as subspecies of *G. kuroiwae* no longer makes sense. Thus, we propose elevating all five taxa currently regarded as subspecies of *G. kuroiwae* to full species, *G. orientalis*, *G. sengokui*, *G. toyamai*, *G. yamashinae*, and *G. yunnu*. Adding *G. splendens* in Tokunoshima and the two species in Okinawajima, there are now seven extant and one extinct species exist in the Ryukyu *Goniurosaurus*.

Key words: Central Ryukyus; *Goniurosaurus nebulozonatus* new species; Eyelid gecko; Parapatry; Taxonomy

Introduction

The genus *Goniurosaurus* Barbour, 1908 is a group of East Asian eyelid geckos, currently consisting of 26 extant species or subspecies (Grismer et al., 1994, 1999; Zhu et al., 2021). The species in the central part of the Ryukyu Archipelago (Central Ryukyus) in Japan are geographically isolated approximately 1,500-km away from the remaining congeners in the northern part of Vietnam and the southern part of China and form a monophyletic group. In the comprehensive taxonomic revision of the Ryukyuan *Goniurosaurus*, based on morphology, Grismer et al. (1994) recognized five allopatric taxa, namely, *G. k. kuroiwae* (Namiye, 1912) (in Okinawajima, Kourijima, and Sesokojima), *G. k. orientalis* (Maki, 1931) (in Tonakijima, Tokashikijima, Akajima, and Iejima), *G. k. yamashinae* (Okada, 1936) (in Kumejima), *G. k. toyamai* Grismer, Ota & Tanaka, 1994 (in Iheyajima), and *G. k. splendens* (Nakamura & Uéno, 1959) (in Tokunoshima). In their analysis Grismer et al. (1994) treated specimens from an island as a single operational unit but they noted that *G. k. kuroiwae* showed considerable variation in dorsal patterns even within Okinawajima.

Subsequent molecular phylogenetic analyses of the Ryukyuan *Goniurosaurus* by Ota et al. (1999) and Honda (2002) depicted a different figure for population relationships. Their analyses based on mitochondrial DNA (mtDNA) sequences revealed that populations from Okinawajima are paraphyletic with respect to the Iejima population of *G. k. orientalis*. Honda et al. (2014), which incorporated samples of all five subspecies from eight geographically distinct areas, further confirmed the close phylogenetic relationship of populations from southern Okinawajima and Iejima, and clearly differentiated the Iejima population from those of Tonakijima and Tokashikijima, of which the former is the type locality of *G. k. orientalis*. They also revealed a large genetic divergence of *G. k. splendens* from the remaining taxa and proposed recognizing it as full species status, *G. splendens*. Honda and Ota (2017) further separated the Tokashikijima and Akajima populations from *G. k. orientalis* as *G. k. sengokui* based on morphological differences, and argued that the Iejima population should be recognized as *G. k. kuroiwae* due to its small mtDNA divergence from southern Okinawajima populations. Nakamura et al. (2014) reported bone remains of *Goniurosaurus* from Yoronjima Island, which was morphologically distinct from any extant species/subspecies, and described it as *G. k. yunnu*, a possibly extinct taxon. Thus, two species and six subspecies have been recognized in the Ryukyuan *Goniurosaurus*, but the taxonomic status of the northern and southern Okinawajima populations remains unresolved (Fig. 1).

Kurita et al. (2018) conducted phylogenetic and population genetic analyses of many local samples within Okinawajima and adjacent islands using mitochondrial and nuclear DNA makers. Their results confirmed the north–south differentiation within *G. k. kuroiwae*, and the two genetically diverged entities are distributed in parapatry in Okinawajima and a few small islands close to Okinawajima (Fig. 1; [1]–[9] versus [12]–[24]) with a hybrid zone in the north-central part of the island (Fig. 1; [9] and [10]). Hybrid genotypes were detected only in a restricted area and the range of the putative hybrid swarm was estimated to be no more than 9 km in the north–south direction. Kurita et al. (2018) argued that the two entities deserved recognition as separate biological species. Their analyses also confirmed the close genetic relationship of the Iejima population (Fig. 1; [24]) to the southern Okinawajima population in the nuclear makers.

In this study, we first conducted genome-wide single nucleotide polymorphism (SNP) analyses to ensure the genetic difference between the northern and southern populations of *Goniurosaurus* spp. in Okinawajima. These genome-wide SNP analyses explained the evolutionary trajectory of *G. k. kuroiwae* in a phy-

* Corresponding author.
E-mail address: mofumofu_monticola@hotmail.co.jp

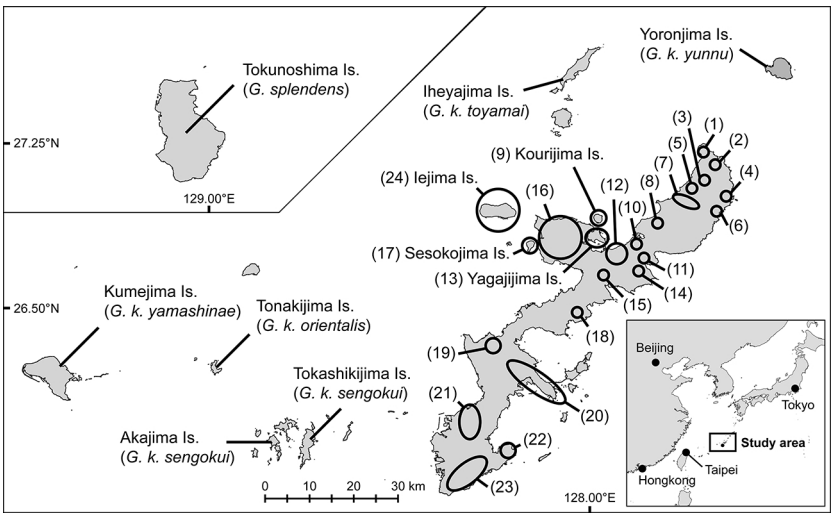

Fig. 1. Eleven islands in the Central Ryukyus where the extant and extinct *Goniurosaurus* geckos are recorded. Circles on Okinawajima and adjacent islands indicate the localities of the examined individuals (specimens and photographic records) of *G. k. kuroiwae* sensu lato with the numerals in parentheses corresponding to those in Table 3.

logenetic context. The qualitative, meristic, and morphometric characters of external morphology were then examined. Simple machine learning algorithms were adopted to explore the discriminant powers of these characteristics. The results of these analyses provided additional support for the distinctiveness of the northern and southern entities, and thus we revised their taxonomic treatment accordingly.

Materials and Methods

Genetic Analyses

SNP data were obtained for all known island populations of the Ryukyuan *Goniurosaurus* except for the Yagajijima, Sesokojima, and Kourijima populations. Populations of the first two islands are close to those in southern Okinawajima, and the last one is close to northern Okinawajima populations (Kurita et al., 2018). Forty-eight geckos whose sampling localities geographically covered all of Okinawajima were used. These samples were picked up from six areas (Fig. 1; [1]+[2], [10], [11], [12]+[15], [16], and [22]+[23]), which included all of the northern lineage ([1]+[2]), hybrid swarms ([10] and [11]), and the southern lineage ([12]+[15], [16], and [22]+[23]) recognized by the results of clustering analyses based on simple sequence repeat markers conducted in the previous study (Kurita et al., 2018). An additional 52 geckos representing other Ryukyuan species/subspecies were also incorporated into the analysis. Eight geckos were examined for each geographical or subspecies sample except for the *G. k. sengokui* sample from Akajima for which only four geckos were available. In total, 100 geckos from 13 areas were used (see Appendix I). A reduced representation sequencing library was prepared using genotyping by random amplicon sequencing, direct (GRAS-Di) technology (Toyota Motor Corporation, Japan) by outsourcing to Bioengineering Lab. Co., Ltd. In summary, short DNA fragments were randomly amplified from total DNA using high-concentration primers with random 3-bp nucleotides at the 3'-end of the oligo (Hosoya et al., 2019), and sequenced with a 150-bp paired-end using Nextseq 500 (Illumina).

Raw sequences were quality checked using FastQC (Andrews, 2010). An adapter sequence

was removed and a low quality portion with <Q20 in the 4-bp sliding-window average was trimmed from the 3'-end for each read. Then, reads with a 30% or more low-quality portion (<Q20), with five or more N sites, with lengths shorter than 80 bp after trimming, or unpaired reads were discarded using Fastp (Chen et al., 2018). The de novo assembly of reduced-representation loci was built using the stacks pipeline (Catchen et al., 2013), in which a 4-bp distance (5% of each one sequence of a pair) between stacks was allowed and at least 8× coverage was required for stack depth. SNPs that satisfied the following conditions were selected using the "populations" function of stacks: the sites that were genotyped in ≧75% of individuals for all the areas, for which the observed heterozygosity and minor allele frequency were <0.6 and >0.01, respectively. Subsequently, further locus and individual filtering was conducted using PLINK 2.0 (Chang et al., 2015) in three steps: individuals and loci with ≧90% missing values were excluded first, then those with ≧80% missing were discarded, and finally loci with ≧30% missing and minor allele frequency <0.02 were removed.

Spatial–genetic structure, including the hybrid zone, was visualized as a phylogenetic network based on an uncorrected-p distance with the neighbor-net method implemented in SplitsTree (Huson and Bryant, 2006). Clustering analyses were conducted using ADMIXTURE (Alexander et al., 2009), where the maximum convergence criterion and the number of iterations were set to 0.0001 and 100, respectively. The number of clusters K was changed from 1 to 15, which is larger than the number of examined areas. Ten independent runs were performed, checking for K with the lowest cross-validation error on average and in all trials. A maximum likelihood tree was reconstructed based on a general time reversible model with ascertainment bias correction, and the reliabilities of internal branches were evaluated by ultrafast bootstrap (Hoang et al., 2018) with 1,000 replicates and SH-aLRT (Guindon et al., 2010) with 1,000 replicates using IQ-Tree (Nguyen et al., 2015). Internal branches with ultrafast bootstrap ≧95 and SH-aLRT ≧80 were regarded as reliable (Minh et al., 2022). Individuals collected from areas occupied by hybrid swarms were removed from this analysis because tree-based clustering analysis is unsuitable for hybrid swarms.

Morphological characters examined

We examined the morphometric, meristic, and qualitative characters of preserved specimens deposited in the Okinawa Prefectural Museum and Art Museum (OPM), the Zoological Collection of Kyoto University (KUZ), the National Museum of Nature and Science (NSMT), and Satoshi Tanaka's Private Collection (TPN) maintained in the OPM. The specimens examined are shown in Appendix 2: in summary 35 specimens of the northern Okinawajima lineage and 143 of the southern Okinawajima lineage including six Iejima specimens of *G. k. kuroiwae*, 47 *G. k. sengokui* from Tokashikijima, two *G. k. sengokui* from Akajima, seven *G. k. orientalis*, six *G. k. yamashinae*, four *G. k. toyamai*, and 15 *G. splendens*. To supplement color pattern data, photo images accumulated during field surveys in 2010–2022 were used. These photo images were assigned to local samples according to the geographical ranges of genetic groups recognized by Kurita et al. (2018), being 238 geckos from northern Okinawajima, 44 from hybrid swarms, 225 from southern Okinawajima, 65 from Iejima, 114 and 17 *G. k. sengokui* from Tokashikijima and Akajima, respectively, 44 *G. k. orientalis*, 75 *G. k. yamashinae*, 17 *G. k. toyamai*, and 48 *G. splendens*. These field surveys and collection of specimens were carried out under the permissions of the Ministry of the Environment of Japan, the Kagoshima Prefectural Boards of Education, and Okinawa Prefectural Boards of Education because all Ryukyuan *Goniurosaurus* species are strictly protected by national laws and the prefecture's ordinance.

The following morphometric characteristics were measured on the left side of specimens using dial calipers accurate to the nearest

0.1 mm: snout–vent length (SVL; from tip of snout to cloaca), head length (from tip of snout to bony tip of occiput), head width (widest part of head), head depth (deepest part of head), snout length (from tip of snout to anterior edge of orbit), eye diameter (diameter of eye opening in anterior–posterior direction), interorbital width (narrowest part of frontal bone), nape width (narrowest part of nape), axilla–groin length (from posterior edge of forelimb insertion to anterior edge of hind limb insertion), brachial length (from forelimb insertion to elbow), forearm length (from elbow to base of the palmar), femur length (from hind limb insertion to knee), and crus length (from knee to base of the sole). These characteristics were measured on the right side only if the left side was damaged.

Observations of scale conditions or counts were made with the aid of a microscope when necessary. The meristic characters examined were the number of supralabials (from scale bordered by rostral to posterior-most scale at least two-times larger than surrounding scales), infralabials (from scale bordered by mental to posterior-most scale at least two-times larger than surrounding scales), scales bordering the nasal scales (including rostral and supralabials), internasals (scales between supranasals and bordered by rostral), postinternasals (granular scales bordered by internasals), postmentals (scales bordered by mental except the first infralabials), postpostmentals (scales posteriorly bordered by postmentals), eyelid fringe scales (enlarged scales surrounding eye opening), snout scales (from scales bordered by posterior edge of supranasal to those bordered by anterior edge of eye opening), scales around a dorsal tubercle (granular scales bordered by a tubercle on dorsum), mid-body tubercle rows (transverse tubercle rows at mid-body), mid-body granular scales (transverse granular scale rows at mid-body), paravertebral tubercles (tubercles at paravertebral lines between axilla-groin part), mid-dorsal stripe I–IV scales (scales corresponding to width of mid-dorsal stripe I–IV; see the next paragraph for the definition of mid-dorsal stripes I–IV and dorsal bands I–IV), dorsal band I–IV scales (scales corresponding to width of transverse bands on dorsum I–IV), tubercles on the dorsal band IV edge (series of bright tubercles on bright colored granular scale patch at dorsal side of hind limb insertions), ventral scales (from postmentals to scales bordered by cloaca), postcloacal scales (from scales bordered by cloaca to those bordered by the first segment of tail), subdigital scales on the fourth fingers (ventral scales of fourth fingers), subdigital scales on the fourth toes (ventral scales of fourth toes), scales around a femur tubercle (scales bordered by a tubercle on dorsal surface of femur), and femur tubercle contacts (numbers of contact points of two neighboring tubercles on femur). The qualitative character examined was the condition of scales on the sole (condition of the largest scales on sole, assigning to any of "no enlarged scale [coded as 0]," "a single largest scale [1]," or "multiple largest scales [2]"). Bilateral characters were counted on both sides of the body, and larger values were used for comparison. For granular scales around the tubercles, nine tubercles were arbitrarily selected, and the median was used. Mid-body tubercle rows, dorsal stripes I–IV scales, and dorsal bands I–IV scales were counted for three different parts and the median values were used.

According to Grismer et al. (1994) the components of the dorsal pattern were treated separately as a lineate mid-dorsal element, transverse banding element, hind limb banding element, and interspace mottling element. They considered that these character states are derived, thus characterizing each taxon or clade: the presence of mid-dorsal stripe for *G. k. kuroiwae*, *G. k. orientalis*, and *G. k. sengokui*, the incomplete transverse bands for *G. k. kuroiwae*, the extension of the posterior most band to hind limbs for *G. splendens*, and the lack of interspace mottling for *G. splendens* and *G. k. toyamai*. Among these elements, we focused on the mid-dorsal stripe and dorsal banding because these characters show some (probably regional) variations within Okinawa-jima; the northernmost populations sometimes

possess faded mid-dorsal stripe and irregular transverse bands, and the southern Okinawa-jima, Sesokojima, and Kourijima populations usually show obvious mid-dorsal stripe and the complete absence or incompleteness of transverse bands (Grismer et al., 1994).

We typified the mid-dorsal stripe and transverse bands by partitioning them into multiple parts and evaluating the presence/absence or completeness of each part. Except for *G. splendens*, the Ryukyuan *Goniurosaurus* usually possesses four transverse bands between the nape and the base of the tail (though sometimes just rudimentary). An additional band at the occipital region that connects auditory meatuses is frequently present in some areas. The bands were defined at the levels of the occipital region, forelimb insertion, anterior part of the trunk, posterior part of the trunk, and base of the tail as the nuchal loop, dorsal band (DB) I, II, III, and IV (DBs-I–IV), respectively. With respect to the mid-dorsal stripe, it may extend from the level of the nuchal loop to that of DB-IV but may exist at only a part in some geckos. The mid-dorsal stripe was divided into four sections according to the levels of the five transverse bands, and referred to as mid-dorsal stripes I, II, III, and IV (MS-I–IV) from the head side to the tail side. The condition of the stripe at each section was evaluated as "absent (coded as 0)," "incomplete (from the short lineate elements to somewhat continuous stripe interrupted partially) (0.5)," or "absent (1)."

The condition of the nuchal loop was classified into four categories: "absent (coded as 0)," "rudimentary (light colored patches exist on dorsal side of auditory meatus only) (1)," "obviously patched (light colored patches occupy <1/2 width of occipital region) (2)," and "present (those occupy ≧1/2 width) (3)." DBs-I–IV were assigned to "absent (coded as 0)" or "present (1)": it was judged as present when it extended ≧1/2 of body width for DBs-I–III and when it covered entire width of body for DB-IV. Note that tubercles on the DB-IV edge were counted even when DB-IV did not exist completely. Three additional characteristics, i.e., the lateral extension of DB-I, the lateral extension of DB-IV, and the sharpness of stripes/bands, were evaluated. The lateral extension of DB-I was categorized into three states: "no extension (not contact to the dorsolateral stripes) (coded as 0)," "swollen shape (contact to the dorsolateral stripes, forming a knob) (1)," or "contact with forelimb insertions (extending beyond dorsolateral stripes) (2)." The extension of DB-IV was categorized as "unextended (coded as 0)" or "extended (exceeding hind-limb insertion base) (1)." The sharpness of stripes/bands was judged as "sharp (coded as 1)" when the edge of the stripe/band shifted to a dark ground color within two granular scales but "diffused (0)" if the transition zone was wider than two granular scales.

Morphological analyses

Random forest decision tree models were constructed for the morphological discrimination of the northern and southern lineages to evaluate the reliability of morphology-based identification and explore the characters useful for their diagnosis. Three experiments with different settings were conducted. In each experiment, 100 independent models were iteratively generated. In each iteration the individuals used for the training and those for the test were randomly selected. The meristic and qualitative (converted to dummy numbers) characteristics were used as variables for modeling, and the interactions between the variables were not considered in these models.

In the first experiment (Experiment 1) models were trained using 18 meristic and 13 qualitative characteristics of 30 northern and 30 southern lineage specimens and subsequently tested by the other five specimens from each lineage. Iejima individuals were removed from this evaluation due to the small sample size. Among the 28 meristic characters listed in the last subsection, mid-body granular scales and ventral scales were excluded from the analysis because the abdominal part of many specimens were previously dissected and thus it was difficult to determine character states for these

specimens exactly. Mid-dorsal stripe I–IV scales and dorsal band I–IV scales were also not included because many specimens lacked stripes and/or bands and thus to be missing for these characters.

The second experiment (Experiment 2) constructed models using the 13 qualitative characters taken from specimens and photo images for 50 individuals from each of the northern, southern, and Iejima populations, and tested using the other 20 individuals from each. In the third experiment (Experiment 3) we considered individual assignment to the lower geographical assemblage level. The northern and southern lineages were strictly separated in this analysis the same as we did in Experiments 1 and 2. On the other hand the operational geographical assemblages did not strictly follow the mitochondrial DNA sublineages recognized by Kurita et al. (2018) in order to keep the sample sizes above a certain level and the differences between groups small for analytical reasons, while reflecting the sublineage distributions. The same character set as Experiment 2 was used. Models were constructed using 30 individuals from each geographic assemblage (five, six, and one from the northern lineage, southern lineage excluding Iejima, and Iejima, respectively) and then tested by the other 10 individuals from each. In the accurate assignment evaluation, 10 individuals from Kourijima, where the population genetically belongs to the northern lineage (Kurita et al., 2018), were also incorporated. Kourijima individuals were excluded from the training process due to the small sample size, and we evaluated how accurately the 10 individuals were assigned to respective assemblages in the "northern" area. Morphological assignment tests were conducted using the caret 6.0.93 (Kuhn, 2008) and randomForest 4.7.1.1 (Liaw and Wiener, 2002) packages in R 4.2.0 (R Core Team, 2022). For Experiments 1 and 2, the importance of characteristics was evaluated based on the mean decrease in Gini impurity using the Boruta algorithm. It was carried out by 1,000 independent iterations of shadow-variable generations and training-individual selections and tested the significance of the contribution of each character at a significance level of 0.01 after Bonferroni's multiple testing adjustments. These tests were conducted using the Boruta 8.0.0 package (Kursa and Rudnicki, 2010).

The morphological variation of *G. k. kuroiwae* was visualized by principal component analysis (PCA), conducted by the "prcomp" function implemented in stats 4.2.0 package (R Core Team, 2022), using characteristics except for those with no contribution to species discrimination according to Boruta tests. Morphological similarities/dissimilarities among geographic samples were summarized in a heat map of the rate of confusion of sampled area.

Results

Spatial–genetic structure of the Ryukyu Goniurosaurus

Approximately 72 million raw reads were obtained for 100 individuals. Because of quality controls and SNP selections, 1,574 loci of 86 individuals from 13 populations remained, where at least two individuals were kept for each population and 12.8% of the sample–locus cells in a matrix were missing (3.2–45.7% of loci were missing for each sample).

Except for the two hybrid swarms, Motobu, and Tokashikijima populations, the neighbor-net network aggregated the members of each population into a separate tip distinguished from the remaining tips (Fig. 2A). The Nago, Motobu, Iejima, and Nanjo populations were genetically close, and the hybrid swarm populations were placed between the Nago–Nanjo and Kunigami populations. The Motobu population was located at the base of the Iejima population. The ADMIXTURE analyses preferred K=9 or 12 on average or minimum, respectively (Fig. 2B). In K=9, *G. k. kuroiwae* populations were separated into four clusters; the Kunigami, Nago, Iejima, and Nanjo populations were assigned to their own clusters, while the hybrid swarms and Motobu populations were expressed as a hybrid between the Kunigami and Nago populations and that

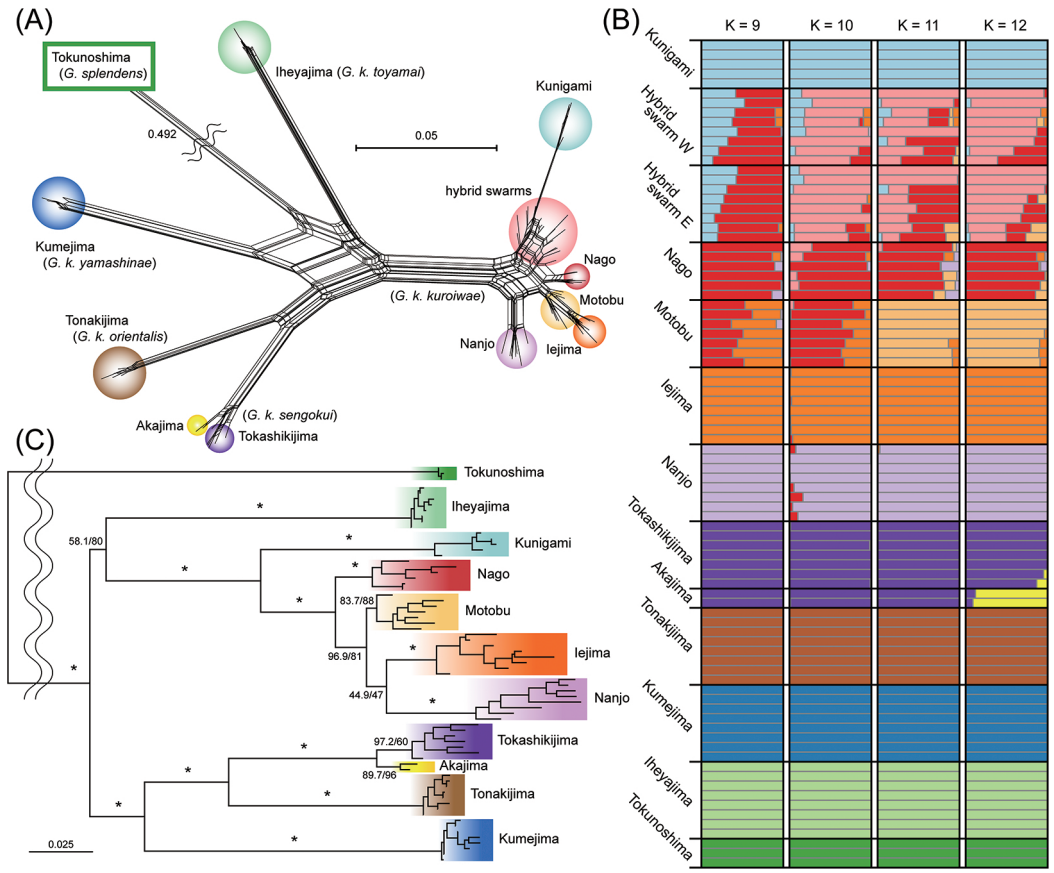

FIG. 2. The phylogenetic network (A), clusters suggested by ADMIXTURE analyses (B), and maximum likelihood tree (C) of *Goniurosaurus* geckos in the Ryukyus. Asterisks in the phylogenetic tree indicate the internal branches with high support values (ultrafast bootstrap ≧95% and SH-aLRT ≧90%).

between the Nago and Iejima populations, respectively. Geckos from the hybrid swarm populations formed a unique cluster by themselves in K=10, but several geckos were judged as "hybrids" between the unique hybrid-swarm cluster and the Nago cluster in the higher Ks. From K=11, geckos from the Motobu population also formed their cluster. The remaining species and subspecies were allocated to their clusters throughout K=9–12. In K=12, the Tokashikijima and Akajima populations of *G. k. sengokui* were separated.

In the maximum likelihood tree analysis, individuals of each of the six taxa formed a monophyletic group supported by enough ultrafast bootstrap and SH-aLRT values (Fig. 2C; ultrafast bootstrap=100/SH-aLRT=100). *Goniurosaurus splendens* was set to the outgroup because of its significant divergence from the other samples. The relationship among the subspecies of *G. kuroiwae* was unsolved except for the monophyly and relationships of *G. k. yamashinae*, *G. k. orientalis*, and *G. k. sengokui* (96.8/99). Among these three subspecies, *G. k. yamashinae* diverged first and *G. k. orientalis* and *G. k. sengokui* were inferred as a sister relationship with significant support (99.8/100). For *G. k. kuroiwae*, the monophyly of each local population, except for the Motobu population, was strong-

ly supported (100/100). Among these populations, the Kunigami population first diverged from the remaining, followed by the Nago population. The relationship among the Motobu, Iejima, and Nanjo populations remained unresolved. The genetic divergence of the Kunigami population from the populations from the Nago to Nanjo region including Iejima was clear, supporting Kurita et al.'s (2018) view that two genetically divergent entities co-occur within Okinawajima.

Accuracy of the morphological assignment of species/population using random forest models

The results of morphological analyses using random forest decision tree models are summarized in Table 1. With respect to Experiment 1 (based on 31 characters), 96.2% of the specimens was accurately identified as their lineages. As a result of character importance evaluation, 13 characters were inferred as significantly contributing to the discrimination of the lineages ($p<0.01/31$; characters marked by "S" in the RF column of Table 2), of which enlarged scale on the pes base, MS-III, and sharpness of stripes/bands edge always showed a higher contribution than shadow variables.

In Experiment 2 (based on 13 characters that could be examined using photo images), the overall accuracy of identification was 86.1%, in which the assignment accuracy was lowest in the northern lineage and highest in the southern lineage excluding the Iejima population. Eleven characters significantly contributed to discriminating the northern Okinawajima, southern Okinawajima, and Iejima populations ($p<0.01/13$; "P" in Table 2), of which MSs-III and IV, nuchal loop, DBs-II and III, lateral extension of DB-I, tubercles on the DB-IV edge, and sharpness of stripes/band edge always showed higher importance than shadows. PCA based on the 13 scalation and dorsal-pattern characters and the 11 significant characteristics on the dorsal patterns showed morphological differences among the northern lineage, the Okinawajima populations of the southern lineage, and the Iejima populations (Fig. 3).

The results of the individual assignment to the population level (Experiment 3) are summarized in Table 1 (population-level labeling), as well as the heat map of the rate of confusion in Fig. 4 to show the pairwise level of correct/incorrect assignments. The accuracy of the population assignment was generally low, from 15.7% for S1 to 52.0% for N1, except for 86.1% for the Iejima population. Most incorrect assignments to different populations happened among populations of the same lineage; indeed, the overall accuracy of lineage-level assignment (whether an individual was assigned to populations of the correct lineage) achived 82.9%. The accuracy of assignment to lineages tended to be high in the northern and southern extremities of Okinawajima and low in the intermediate region, especially low in the Kourijima population (18.9%).

Taxonomic conclusion and description of a new species

The northern and southern lineages were distinguished genetically and morphologically, as shown in the previous sections. These results of remarkable north–south differentiation in Okinawajima were compatible with those of Kurita et al. (2018), lending additional support to the view that the northern and southern lineages of *G. k. kuroiwae* are two separate species. The type locality of *G. kuroiwae*, and thus that of nominotypical subspecies, is Mt. Taniyo-dake (now called Tano-dake), Haneji, Nago City, Okinawajima (Namiye, 1912), which is within the range of the southern species, indicating that the species name *Goniurosaurus kuroiwae* (Namiye, 1912) should be assigned to the southern species. Morphological observation of the holotype also agreed with this view (see below).

It is clear that the northern species differs from all extant nominal species/subspecies (see above). The northern species was not compared with *G. k. yunnu* in this study. However, Nakamura et al. (2014) made direct comparison of *G. k. yunnu* with samples from Kunigami (apparently within the range of the northern species) and showed their difference in the

TABLE 1. The probability that an individual collected from an area occupied by a respective genetic lineage is assigned to each predicted source area under three random forest decision tree models. For the analyses with the population-level labeling, two genetically distinct lineages, namely the northern and southern lineages, were taken into account when pre-defining the population, while priority was given to the geographical proximity of individuals and the balance of sample sizes in the predefined population rather than to more subordinate genetic structures (see the Materials and Method section for detail). N indicates the number of individuals used for the validations.

	N	North	South	Iejima	Source area accuracy	Overall accuracy**
Species-level labeling						
Specimen only* (Experiment 1)						0.962
Northern lineage	35	0.962	0.038	—		
Southern lineage	135	0.038	0.962	—		
Specimen+Photo (Experiment 2)						0.861
Northern lineage	273	0.789	0.074	0.138		
Southern lineage	362	0.068	0.919	0.014		
Iejima population	71	0.102	0.022	0.876		
Population-level labeling						
Specimen + Photo (Experiment 3)						0.829
N1	74	0.867	0.007	0.126	0.520	
N2	52	0.890	0.098	0.012	0.163	
N3	48	0.973	0.012	0.015	0.332	
N4	48	0.833	0.158	0.009	0.313	
N5	41	0.775	0.217	0.008	0.347	
N6 (Kourijima)	10	0.189	0.758	0.053	—	
S1	46	0.199	0.801	0.000	0.157	
S2	64	0.133	0.820	0.047	0.307	
S3	46	0.172	0.818	0.010	0.248	
S4	86	0.080	0.915	0.005	0.201	
S5	62	0.030	0.914	0.056	0.534	
S6	58	0.016	0.984	0.000	0.286	
S7 (Iejima)	71	0.116	0.023	0.861	0.861	

* Except for the Iejima population

** At species level (Northern lineage versus Southern lineage, including the Iejima population in the analyses based on specimens and photographs)

shapes of maxillary and frontal bones and the number of maxillary teeth. There are no synonyms under the nominal taxa of genus *Goniurosaurus*; therefore, the northern species is considered undescribed. We describe it as a new species and also provide the redescription of *G. kuroiwae* in the following section.

In association with recognizing the northern and southern lineages as full species, all other extant taxa of the Ryukyuan *Goniurosaurus* should be raised to full species, *G. splendens*, *G. orientalis*, *G. yamashinae*, *G. toyamai*, and *G. sengokui*. Considering the phylogenetic relationships and levels of genetic divergence among these taxa and the two species in Okinawajima, placing any taxa as subspecies of *G. kuroiwae* (and of other species) does not make sense anymore. Although the phyloge-

TABLE 2. Measuremens, scalation, and dorsal pattern of *Goniurosaurus* geckos in the central Ryukyus. The letters "X", "S", and "P" in the RF column indicates the variables included to random forest models but are inferred not to contribute to discrimination between *G. nebulozonatus* and *G. kuroiwae* by the Boruta algorithm, that with a significant importance in models constructed based on scalation and dorsal pattern, and that with a significant importance in models based on dorsal pattern only, respectively.

Characters	RF	*Goniurosaurus nebulozonatus* sp. nov.	Holotype of *G. nebulozonatus*	Hybrid swarms	*G. kuroiwae* (excluding Iejima)	Holotype of *G. kuroiwae*	*G. kuroiwae* (Iejima)	*G. sengokui*	*G. orientalis*	*G. yamashinae*	*G. toyamai*	*G. splendens*
Snout–vent length		80.0±10.1 (54.9–93.9; n=35)	79.8		78.0±9.2 (46.7–93.2; n=137)	50.2	67.5±23.0 (37.5–88.2; n=6)	76.7±10.6 (47.7–91.0; n=49)	81.9±19.3 (47.8–96.8; n=7)	74.7±8.7 (58.8–83.5; n=6)	84.5±2.5 (82.1–87.8; n=4)	75.4±3.9 (67.2–82.1; n=15)
Head length		21.5±2.2 (14.9–24.2; n=35)	20.8		20.6±2.4 (12.5–24.7; n=137)	15.0	17.8±5.0 (11.4–21.9; n=6)	18.4±2.3 (12.0–23.3; n=49)	21.4±3.7 (14.8–24.4; n=7)	19.7±2.1 (15.8–22.2; n=6)	23.1±1.7 (22.0–25.7; n=4)	18.5±3.1 (7.8–20.9; n=15)
Head width		14.4±1.7 (9.2–16.6; n=35)	14.3		13.9±1.7 (8.5–20.9; n=137)	10.2	12.3±3.9 (7.1–16.1; n=6)	13.8±2.3 (8.3–21.9; n=49)	14.6±3.7 (8.6–18.0; n=7)	14.0±1.9 (10.4–15.8; n=6)	16.8±0.9 (16.1–18.1; n=4)	13.1±0.7 (11.5–14.0; n=15)
Head depth		9.4±1.1 (6.2–11.3; n=35)	8.9		8.9±1.1 (5.3–13.9; n=137)	5.9	7.7±2.4 (4.4–9.8; n=6)	8.6±1.4 (5.1–11.1; n=49)	9.2±2.5 (5.2–12.1; n=7)	8.8±1.5 (6.3–10.3; n=6)	10.7±0.5 (10.4–11.4; n=4)	8.1±0.6 (6.9–9.2; n=15)
Snout length		8.0±0.9 (5.2–9.3; n=35)	7.6		7.7±0.9 (4.8–9.0; n=137)	5.5	6.7±2.1 (3.8–8.4; n=6)	7.7±1.0 (5.0–9.3; n=49)	8.0±1.7 (5.1–9.3; n=7)	7.5±1.1 (5.6–8.8; n=6)	8.7±0.6 (8.2–9.5; n=4)	7.3±0.3 (6.7–7.7; n=15)
Eye diameter		5.4±0.6 (3.7–6.3; n=35)	5.2		5.1±0.7 (2.7–6.5; n=137)	3.9	4.6±1.2 (3.0–5.6; n=6)	4.5±0.7 (2.8–6.0; n=49)	5.3±1.1 (3.5–6.3; n=7)	5.1±0.8 (3.9–6.5; n=6)	5.7±0.5 (5.0–6.1; n=4)	4.9±0.3 (4.4–5.3; n=15)
Interorbital width		2.8±0.4 (1.7–3.1; n=35)	2.7		2.7±0.3 (1.7–3.3; n=137)	1.9	2.6±0.8 (1.5–3.2; n=6)	2.6±0.4 (2.2–3.3; n=6)	3.0±0.8 (1.9–3.9; n=7)	3.4±1.4 (2.6–6.2; n=6)	3.2±0.2 (3.1–3.4; n=4)	2.6±0.2 (2.2–2.9; n=15)
Nape width		7.9±1.2 (5.1–10.0; n=35)	8.1		7.6±1.0 (4.5–9.5; n=137)	6.0	6.9±2.5 (3.7–9.4; n=6)	7.5±1.4 (6.2–10.1; n=6)	8.4±2.4 (4.3–11.0; n=7)	8.4±1.4 (5.7–9.6; n=6)	9.6±0.4 (9.1–10.1; n=4)	7.0±0.8 (5.5–8.5; n=15)
Axilla–groin length		35.3±5.6 (22.5–46.9; n=35)	37.1		34.1±4.6 (19.4–44.4; n=137)	20.1	31.7±11.8 (16.2–43.5; n=6)	35.6±3.6 (31.8–42.4; n=6)	38.6±10.0 (20.8–49.3; n=7)	32.7±4.4 (26.9–37.3; n=6)	35.9±1.7 (34.7–38.4; n=4)	35.3±3.2 (27.7–39.6; n=15)
Brachial length		9.8±1.3 (6.8–12.9; n=35)	10.2		9.4±1.3 (5.3–12.4; n=137)	6.7	9.5±3.2 (5.3–12.4; n=6)	9.9±1.2 (8.4–11.2; n=6)	11.5±2.7 (7.4–13.7; n=7)	10.6±1.3 (8.5–12.5; n=6)	11.0±0.6 (10.6–11.9; n=4)	10.2±0.8 (8.8–11.6; n=15)
Forearm length		12.5±1.7 (7.9–15.6; n=35)	13.0		11.6±1.6 (6.0–13.9; n=137)	8.0	10.9±3.5 (6.1–13.6; n=6)	11.4±1.3 (9.6–13.5; n=6)	12.7±2.9 (7.7–15.1; n=7)	12.3±1.4 (9.6–13.4; n=6)	13.8±0.3 (13.4–14.0; n=4)	11.9±0.6 (10.7–13.0; n=15)
Femur length		13.8±1.7 (9.1–16.9; n=35)	13.9		13.1±1.7 (6.9–15.6; n=137)	9.9	11.8±3.9 (7.0–15.7; n=6)	10.9±4.0 (3.3–14.1; n=6)	14.1±3.2 (8.8–16.6; n=7)	13.4±1.5 (10.6–15.3; n=6)	15.4±0.7 (14.7–16.2; n=4)	13.7±0.9 (12.5–15.7; n=15)
Crus length		14.7±1.6 (10.1–17.2; n=35)	14.3		14±1.7 (8.1–16.7; n=137)	10.9	12.0±3.9 (7.0–15.7; n=6)	13.0±1.3 (11.4–15.2; n=6)	14.4±3.1 (9.1–16.8; n=7)	13.8±1.9 (10.5–16.5; n=6)	15.9±0.4 (15.3–16.2; n=4)	13.9±0.4 (13.0–14.5; n=15)
Supralabials	X	9.6±0.8 (8–12; n=35)	9/9		9.6±0.8 (8–13; n=136)	9/9	9.3±0.5 (9–10; n=6)	10.0±0.8 (8–11; n=49)	9.6±0.5 (9–10; n=7)	8.7±0.8 (8–10; n=6)	9.5±0.6 (9–10; n=4)	9.7±0.6 (9–11; n=15)
Infralabials	X	9.1±0.8 (7–10; n=35)	10/10		9.2±0.8 (8–11; n=136)	9/10	9.3±0.8 (8–10; n=6)	9.6±0.9 (8–11; n=49)	9.1±0.4 (9–10; n=7)	8.8±0.8 (8–10; n=6)	9.0±0.8 (8–10; n=4)	9.3±0.8 (8–11; n=15)
Scales bordering nasals	X	9.3±1.1 (8–12; n=34)	10/11		8.7±1.2 (7–12; n=136)	11/12	8.7±1.5 (7–10; n=6)	8.5±0.9 (7–11; n=49)	7.6±1.0 (6–9; n=7)	10.5±0.6 (10–11; n=6)	10.0±0.0 (10–10; n=4)	10.6±0.7 (9–12; n=14)
Internasals	X	1.2±0.5 (1–3; n=35)	3		1.2±0.4 (0–2; n=136)	1	1.0±0.0 (1–1; n=6)	1.1±0.4 (1–2; n=49)	1.6±0.8 (1–3; n=7)	2.0±0.6 (1–3; n=6)	3.0±0.0 (3–3; n=4)	1.2±0.6 (1–3; n=14)
Post-internasals	X	1.8±0.5 (1–3; n=35)	3		1.6±0.6 (0–3; n=136)	1	1.7±0.5 (1–2; n=6)	1.6±0.7 (1–3; n=49)	1.9±0.7 (1–3; n=7)	2.7±0.5 (2–3; n=6)	2.8±0.5 (2–3; n=4)	1.9±0.7 (1–3; n=13)
Postmentals	X	5.3±0.8 (4–7; n=35)	6		5.1±0.9 (3–7; n=135)	5	4.3±1.2 (3–6; n=6)	4.0±0.7 (3–5; n=49)	3.3±0.8 (2–4; n=7)	5.0±0.6 (4–6; n=6)	4.5±0.6 (4–5; n=4)	2.6±0.5 (2–4; n=15)
Post-postmentals	X	8.7±1.1 (7–11; n=35)	8		9.0±1.2 (6–12; n=135)	9	8.2±0.4 (8–9; n=6)	8.5±1.2 (6–11; n=49)	7.4±0.8 (6–8; n=7)	10.0±0.9 (9–11; n=6)	8.0±0.8 (7–9; n=4)	5.7±0.5 (5–6; n=15)
Eyelid fringe scales	X	60.0±3.7 (53–67; n=35)	65/65		60.3±3.1 (53–67; n=137)	61/63	59.5±3.4 (57–66; n=6)	60.9±3.5 (51–68; n=49)	51.7±2.1 (50–55; n=7)	55.0±3.4 (50–58; n=6)	57.8±0.5 (57–58; n=4)	54.0±1.8 (52–58; n=15)
Snout scales	X	23.2±1.6 (20–28; n=35)	25/26		24.2±1.5 (20–28; n=136)	23/23	23.2±0.8 (22–24; n=6)	24.5±1.7 (21–28; n=49)	22.4±1.3 (20–24; n=7)	25.0±2.0 (23–28; n=6)	24.0±2.2 (21–26; n=4)	23.3±1.2 (22–26; n=15)
Scales around dorsal tubercles	X	12.1±0.6 (11–13; n=35)	12 (11–14)		12.4±0.6 (11–14; n=137)	12 (11–14)	12.8±0.4 (12–13; n=6)	12.0±0.6 (11–13; n=24)	11.6±0.5 (11–12; n=7)	12.3±0.5 (12–13; n=6)	12.0±0.8 (11–13; n=4)	10.0±0.0 (10–10; n=15)
Mid-body tubercle rows	S	23.5±1.3 (21–27; n=35)	27 (26–28)		25.4±1.6 (22–29; n=137)	25 (24–25)	23.8±1.5 (22–25; n=6)	23.9±1.3 (21–26; n=24)	23.0±2.0 (20–26; n=7)	24.0±1.4 (22–26; n=6)	25.0±1.4 (24–27; n=4)	20.3±1.5 (18–23; n=15)
Mid-body granular scales		140.2±7.4 (123–151; n=35)	146		142.5±6.0 (128–157; n=86)	134	130.7±6.3 (123–140; n=6)	141.1±7.0 (128–152; n=23)	133.3±8.4 (120–146; n=7)	144.7±4.1 (139–151; n=6)	132.8±10.5 (120–144; n=4)	123.0±6.1 (110–135; n=15)
Paravertebral tubercles	S	27.2±1.6 (24–29; n=35)	29/29		25.3±2.0 (20–30; n=137)	28/27	28.0±1.1 (26–29; n=6)	27.5±1.9 (23–31; n=49)	29.6±1.3 (27–31; n=7)	27.2±0.8 (26–28; n=5)	28.3±2.1 (26–31; n=4)	21.4±1.8 (18–24; n=15)
Ventral scales		192.2±8.9 (172–208; n=35)	197		189.7±8.3 (170–208; n=85)	195	185.3±3.7 (178–188; n=6)	206.6±9.9 (178–226; n=23)	194.6±5.6 (184–202; n=7)	197.4±4.7 (191–202; n=5)	192.5±7.9 (182–201; n=4)	208.3±7.5 (198–226; n=15)
Postcloacal scales	X	16.7±1.9 (12–20; n=35)	14		16.6±1.6 (12–20; n=136)	16	16.5±1.4 (15–18; n=6)	17.5±2.0 (13–21; n=48)	15.6±1.4 (14–18; n=7)	15.8±1.6 (14–18; n=6)	16.5±0.6 (16–17; n=4)	17.5±1.8 (15–20; n=15)

TABLE 2. (continued)

Characters	RF	*Goniurosaurus nebulozonatus* sp. nov.	Holotype of *G. nebulozonatus*	Hybrid swarms	*G. kuroiwae* (excluding Iejima)	Holotype of *G. kuroiwae*	*G. kuroiwae* (Iejima)	*G. sengokui*	*G. orientalis*	*G. yamashinae*	*G. toyamai*	*G. splendens*
Subdigital scales on fourth fingers	S	16.7±1.4 (13–19; n=35)	19/17		15.4±1.0 (12–18; n=136)	13/15	15.2±1.2 (14–17; n=6)	15.2±1.0 (13–19; n=49)	16.0±1.0 (14–17; n=7)	16.3±1.2 (15–18; n=6)	15.3±0.5 (15–16; n=4)	14.7±1.4 (12–17; n=15)
Subdigital scales on fourth toes	X	19.4±1.2 (17–23; n=35)	21/23		19.0±1.1 (17–23; n=137)	17/18	18.3±1.5 (17–21; n=6)	18.6±1.1 (16–21; n=49)	21.0±1.2 (20–23; n=7)	19.5±1.5 (18–22; n=6)	18.3±1.3 (17–20; n=4)	17.8±1.1 (16–20; n=15)
Scales around femur tubercles	S	11.1±0.6 (10–13; n=35)	12 (10–14)		11.8±0.7 (10–13; n=137)	12 (10–13)	11.7±0.8 (11–13; n=6)	12.0±0.6 (10–13; n=24)	12.0±0.8 (11–13; n=7)	12.5±0.6 (12–13; n=6)	11.3±0.5 (11–12; n=4)	10.1±0.5 (9–11; n=15)
Contact of femur tubercles	S	8.9±4.0 (4–20; n=35)	12/16		15.1±5.9 (6–37; n=137)	17/14	19.2±5.9 (13–29; n=6)	5.5±3.1 (1–13; n=24)	2.7±1.6 (1–6; n=7)	8.7±4.4 (0–12; n=6)	6.5±3.4 (3–11; n=4)	1.8±1.2 (0–4; n=15)
Enlarged scales on pes	S	1; 1 (85.7%) (n=35)	1/1		2; 2 (86.9%) (n=137)	1/1	2; 2 (83.3%) (n=6)	2; 2 (93.9%) (n=49)	1; 1 (71.4%) (n=7)	0; 0 (83.3%) (n=6)	2; 2 (100%) (n=4)	2; 2 (100%) (n=15)
Mid-dorsal stripe I	X	1; 1 (72.5%) (n=273)	1	1; 1 (86.4%) (n=44)	1; 1 (94.8%) (n=362)	1	1; 1 (91.5%) (n=71)	1; 1 (62.2%) (n=180)	0.5; 1 (39.2%) (n=51)	0; 0 (88.9%) (n=81)	0; 0 (100%) (n=21)	0.5; 0.5 (65.1%) (n=63)
MS-II	SP	0; 0 (50.9%) (n=273)	0	1; 1 (68.2%) (n=44)	1; 1 (82.3%) (n=362)	1	0.5; 1 (47.9%) (n=71)	0.5; 0 (48.3%) (n=180)	0; 0 (94.1%) (n=51)	0; 0 (98.8%) (n=81)	0; 0 (100%) (n=21)	0.5; 0.5 (61.9%) (n=63)
MS-III	SP	0; 0 (77.7%) (n=273)	0	0.5; 0.5 (52.3%) (n=44)	0.5; 1 (48.9%) (n=362)	0	0; 0 (74.6%) (n=71)	0; 0 (91.7%) (n=180)	0; 0 (98.0%) (n=51)	0; 0 (100%) (n=81)	0; 0 (100%) (n=21)	0.5; 0.5 (63.5%) (n=63)
MS-IV	SP	0.5; 0.5 (50.5%) (n=273)	0	0.5; 0.5 (47.7%) (n=44)	1; 1 (66.3%) (n=362)	0	0; 0 (60.6%) (n=71)	0; 0 (71.1%) (n=180)	0; 0 (100%) (n=51)	0; 0 (100%) (n=81)	0; 0 (100%) (n=21)	0.5; 0.5 (58.7%) (n=63)
Mid-dorsal stripe I scales		5.9±1.4 (3–9; n=35)	8 (6–8)		6.8±1.3 (2–9; n=137)	7 (6–7)	9.3±2.8 (5–12; n=6)	9.3±1.0 (8–11; n=6)	8.0±1.3 (6–10; n=6)	9.3±4.2 (6–14; n=3)		3.8±1.0 (2–6; n=13)
MS II scales		6.0±1.1 (4–8; n=24)			6.1±1.3 (3–10; n=136)	6 (5–6)	7.0±2.0 (5–10; n=6)	6.5±1.0 (6–8; n=4)				3.1±0.8 (2–4; n=14)
MS III scales		6.5±1.5 (4–9; n=8)			6.4±1.5 (2–10; n=127)		10.0±0 (10–10; n=1)					2.9±0.8 (2–4; n=12)
MS IV scales		6.1±1.9 (2–11; n=19)			6.6±1.3 (4–10; n=135)		7.7±1.2 (7–9; n=3)	7.3±1.5 (6–9; n=3)				3.0±0.9 (2–5; n=14)
Nuchal loop	SP	1; 0 (43.2%) (n=273)	1	0; 0 (70.5%) (n=44)	1; 0 (48.2%) (n=361)	0	2; 2 (87.3%) (n=71)	2; 2 (67.2%) (n=180)	3; 3 (66.7%) (n=51)	3; 3 (84.0%) (n=81)	3; 3 (81.0%) (n=21)	3; 3 (98.4%) (n=63)
Dorsal band I	P	0; 0 (81%) (n=273)	1	0; 0 (100%) (n=44)	0; 0 (91.2%) (n=362)	0	1; 1 (69.0%) (n=71)	1; 1 (78.9%) (n=180)	1; 1 (84.3%) (n=51)	1; 1 (98.8%) (n=81)	1; 1 (100%) (n=21)	0; 0 (76.2%) (n=63)
DB-II	SP	1; 1 (65.2%) (n=273)	1	0; 0 (95.5%) (n=44)	0; 0 (97.2%) (n=362)	0	1; 1 (69.0%) (n=71)	1; 1 (100%) (n=180)	1; 1 (100%) (n=51)	1; 1 (98.8%) (n=81)	1; 1 (100%) (n=21)	1; 1 (76.2%) (n=63)
DB-III	SP	1; 1 (74.0%) (n=273)	1	0; 0 (86.4%) (n=44)	0; 0 (92.8%) (n=362)	0	1; 1 (91.5%) (n=71)	1; 1 (100%) (n=180)	1; 1 (100%) (n=51)	1; 1 (100%) (n=81)	1; 1 (81.0%) (n=21)	1; 1 (100%) (n=63)
DB-IV	P	1; 1 (65.2%) (n=273)	1	0; 0 (84.1%) (n=44)	0; 0 (71.3%) (n=362)	1	1; 1 (87.3%) (n=71)	1; 1 (93.3%) (n=180)	1; 1 (100%) (n=51)	1; 1 (98.8%) (n=81)	1; 1 (100%) (n=21)	1; 1 (100%) (n=63)
Lateral extension of DB-I	P	0; 0 (71.8%) (n=273)	1	0; 0 (84.1%) (n=44)	0; 0 (77.9%) (n=362)	0	2; 2 (84.5%) (n=71)	2; 2 (63.9%) (n=180)	2; 2 (68.6%) (n=51)	2; 2 (61.7%) (n=81)	2; 2 (100%) (n=21)	2; 2 (98.4%) (n=63)
Femoral extension of DB-IV	X	0; 0 (98.5%) (n=273)	0	0; 0 (100%) (n=44)	0; 0 (100%) (n=362)	0	0; 0 (81.7%) (n=71)	0; 0 (97.2%) (n=180)	1; 1 (94.1%) (n=51)	0; 0 (96.3%) (n=81)	1; 1 (90.5%) (n=21)	1; 1 (90.5%) (n=63)
Dorsal-band I scales		5.7±1.0 (4–7; n=6)	7 (6–8)		5.9±1.5 (4–9; n=20)		7.5±1.7 (6–10; n=4)	8.0±2.9 (5–12; n=5)	12.9±4.9 (7–20; n=7)	8.8±1.8 (7–12; n=6)	10.3±1.5 (8–11; n=4)	9.3±1.2 (7–11; n=15)
DB II scales		6.2±2.0 (3–11; n=18)	11 (9–12)		6.2±2.5 (2–9; n=6)		8.7±3.8 (6–13; n=3)	9.3±2.1 (6–12; n=6)	13.4±2.4 (10–17; n=7)	8.5±1.2 (7–10; n=6)	10.0±1.2 (9–11; n=4)	
DB III scales		7.3±1.5 (5–11; n=20)	11 (11–12)		6.6±2.0 (4–9; n=7)		10.2±1.9 (8–13; n=5)	10.0±2.0 (7–12; n=6)	15.0±2.2 (12–18; n=7)	9.0±1.8 (7–12; n=6)	9.5±1.7 (7–11; n=4)	9.8±1.3 (7–12; n=15)
DB IV scales		7.8±2.2 (4–12; n=24)	10 (8–13)		8.2±1.3 (5–11; n=53)	7 (6–7)	10.4±3.1 (8–15; n=5)	11.6±2.5 (8–15; n=5)	18.0±1.9 (15–21; n=7)	10.7±1.9 (9–14; n=6)	10.5±1.3 (9–12; n=4)	10.1±1.4 (7–12; n=15)
Tubercles on DB-IV edge	P	3.1±1.4 (0–8; n=273)	4/5	2.2±1.5 (0–5; n=44)	2.3±1.2 (0–6; n=362)	3/3	6.2±1.7 (3–11; n=71)	3.7±1.0 (1–7; n=180)	4.1±1.1 (2–6; n=51)	2.7±0.7 (2–5; n=81)	4.6±1.1 (3–8; n=21)	3.9±0.8 (2–8; n=63)
Sharpness of stripes/bands edges	SP	0; 0 (81.7%) (n=273)	0	0; 0 (65.9%) (n=44)	1; 1 (85.4%) (n=362)	1	1; 1 (95.8%) (n=71)	1; 1 (89.4%) (n=180)	1; 1 (82.4%) (n=51)	1; 1 (96.3%) (n=81)	1; 1 (100%) (n=21)	1; 1 (90.5%) (n=63)

Average and standard deviation, and in parenthesis range and sample size, were shown for morphometric and meristic characters (from snout-vent length to contact of tubercles on femur).

Range of non-bilateral meristic characters that were counted in multiple times or multiple parts indicated the range of median values of examined individuals in each species/populations, but in the holotypes simply showed the range of counts.

Median and mode with proportion of individuals showing the character state in parenthesis were shown, followed by sample size, for quantitative characters (from enlarged scales on sole to extension of DB4 to femur).

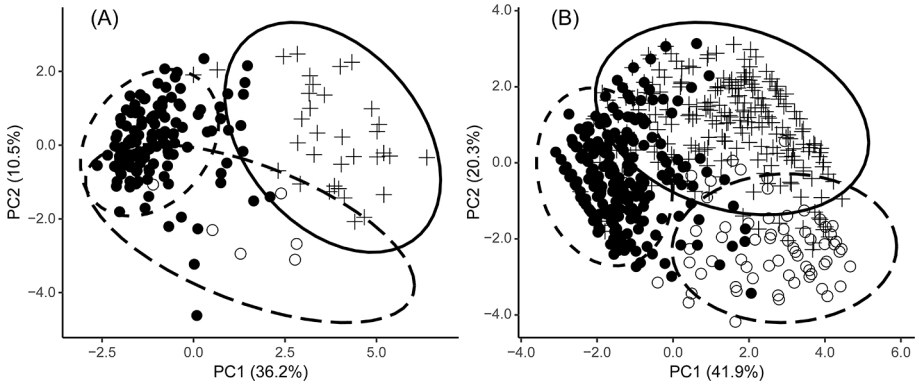

FIG. 3. PCA results based on 13 scalation and dorsal pattern-related characters (A) and 11 dorsal pattern characters (B). Crosses, closed circles, and open circles indicate the northern lineage, southern lineage, and Iejima population of *G. k. kuroiwae* sensu lato, respectively. Solid and dashed ellipses indicate 95% confidence ellipses for the northern and southern lineages, respectively, and those for the Iejima populations and the remaining southern individuals are shown separately.

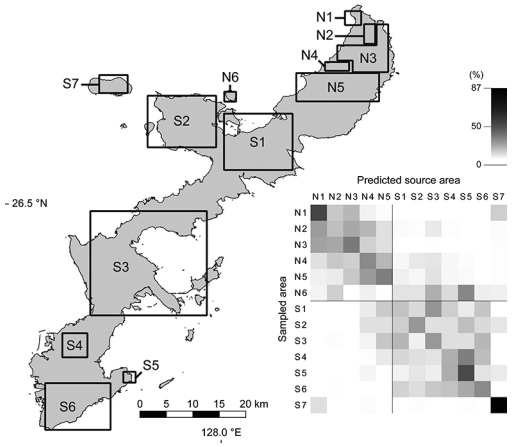

FIG. 4. Population-level labeling of examined individuals for random forest modeling, and a heat map showing the probability that an individual collected from a sampled area is assigned to respective predicted source area in the Experiment 3.

netic position of *G. k. yunnu* is unknown, we also suggest raising it to the full species status, *G. yunnu*, because there is no reason to consider it a subspecies of *G. kuroiwae*.

SYSTEMATICS

Goniurosaurus ***nebulozonatus*** sp. nov.
(Suggested Japanese name: Yambaru Tokage-modoki)

Eublepharis kuroiwae kuroiwae: Nakamura & Uéno, 1963 (in part)
Amamisaurus kuroiwae: Börner, 1981 (in part)
Goniurosaurus kuroiwae: Grismer, 1987 (in part)
Goniurosaurus kuroiwae: Ota, 1989 (in part)
Goniurosaurus kuroiwae kuroiwae: Grismer et al., 1994 (in part)
Goniurosaurus kuroiwae kuroiwae: Nakamura et al., 2014 (in part)
Goniurosaurus kuroiwae kuroiwae: Honda et al., 2014 (as northern Okinawajima population)
Goniurosaurus kuroiwae kuroiwae: Honda and Ota, 2017 (as northern Okinawajima population)
Goniurosaurus kuroiwae: Kurita et al., 2018 (as northern species)

Holotype

KUZ R88884 (Fig. 5), an adult male collected on 19 September 2020 by Takaki Kurita from Oku, Kunigami Village, Kunigami Dis-

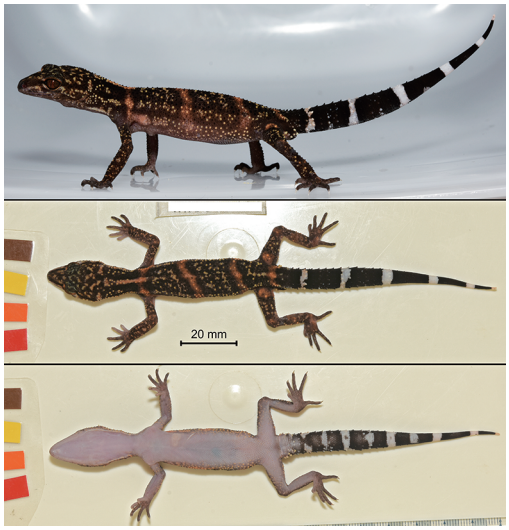

FIG. 5. The holotype of *Goniurosaurus nebulozonatus* (KUZ R88884). Lateral (top), dorsal (middle), and ventral (bottom) views.

trict, Okinawa, Japan (locality [2] in Fig. 1; 26.83460° N, 128.28726° E in WGS84; 10 m above sea level).

Paratypes

KUZ R88885 from Benoki, Kunigami Vil., Kunigami Dist., Okinawa, Japan; OPM H1177, H1670 (two individuals), H1502596–H1502613 (formerly TPN 77050201–77050204, 77052101, 77081804–77081812, 77081911, 77081912, 77082103, and 77082104), and H1502617 (formerly TPN 78042302) from Yona, Kunigami Vil., Kunigami Dist., Okinawa, Japan.

Other specimens/photographic records examined

Specimens: TPN 77082102 from Yona, Kunigami Vil., Kunigami Dist., Okinawa, Japan; OPM H1502618–H1502620 (TPN 78042305, 78042306, and 78042308) and TPN 78042307 from Hentona, Kunigami Vil., Kunigami Dist., Okinawa, Japan; OPM H1043, H1502614–H1502616, H1502548, and H1502549 (TPN 78032701–78032703, 76052401, and 76052406) from Yonaha, Kunigami Vil., Kunigami Dist., Okinawa, Japan. Photographic records: 206 individuals from Kunigami Vil., 22 from Ogimi Vil., and 10 from Kourijima Island.

Diagnosis (Table 2)

A moderate-sized *Goniurosaurus* gecko (ca. 75–95 mm SVL for adults). *Goniurosaurus nebulozonatus*, together with the other six extant species in the Central Ryukyus, is distinguished from continental congeners in having unsheathed claws bordered by, in general, six short, unenlarged scales; in lacking deep axillary pockets; and no precloacal-femoral pores in males. *Goniurosaurus nebulozonatus* is distinguished from all other Ryukyu *Goniurosaurus*, except *G. kuroiwae*, in the combination of the following characters: snout–vent length over 93 mm in maximum [versus 83.5 mm in *G. yamashinae* and 82.1 mm in *G. splendens* (ca. <90% of *G. nebulozonatus* and *G. kuroiwae*)]; iris reddish brown (yellow ocher in *G. orientalis* and *G. yamashinae*); 8–12 scales bordering nasal (6–9 in *G. orientalis*); 4–7 postmentals (3–5 in *G. sengokui*, 2–4 in *G. orientalis*, and 2–4 in *G. splendens*); 7–11 post-postmentals (5–6 in *G. splendens*); 53–67 eyelid fringe scales (50–55 in *G. orientalis*); 11–13 scales around dorsal tubercles (10 in *G. splendens*); 21–27 mid-body tubercle rows (18–23 in *G. splendens*); 123–151 mid-body granular scales (110–135 in *G. splendens*); 24–29 paravertebral tubercles (18–24 in *G. splendens*); ventral scales enlarged, flat, and imbricate (strongly-raised and juxtaposed in *G. splendens*); 172–208 ventrals (198–226 in *G. splendens*); 4–20 femur tubercle contacts (1–6 in *G. orientalis* and 0–4 in *G. splendens*); usually one most-enlarged scale on proximal portion of pes (two or more enlarged scales in *G. sengokui*, *G. toyamai*, and *G. splendens*, and no enlarged scales in *G. yamashinae*); MS-I present in significant portion of individuals (usually absent in *G. yamashinae* and *G. toyamai*, and absent or present as ground-color fading on vertebral line in *G. splendens*); 3–9 granular scales baring MS-I (8–11 in *G. sengokui* and if any

6–14 in *G. yamashinae*); nuchal loop usually absent or incomplete (usually complete in *G. yamashinae*, *G. toyamai*, and *G. splendens*); DB-I absent in most individuals (usually present in *G. sengokui* and *G. orientalis*, and mostly present in *G. yamashinae* and *G. toyamai*); DB-I or rudimentary patch on shoulder usually separated more or less from forelimb insertion by ground-colored space (connecting to forelimb insertion in *G. toyamai* and *G. splendens*); DB-IV not extending to femur (usually extending to femur in *G. orientalis*, *G. toyamai*, and *G. splendens*); 4–7 DB-I scales if any (5–12 in *G. sengokui*, 7–20 in *G. orientalis*, 7–12 in *G. yamashinae*, 8–11 in *G. toyamai*, and 7–11 in *G. splendens*); narrow DBs-II–IV (broad in *G. orientalis*); and diffused edge of stripes/bands (usually sharp in *G. yamashinae*, *G. toyamai*, and *G. splendens*). *Goniurosaurus nebulozonatus* differs from *G. kuroiwae* in satisfying more than half of the following five character states: usually 10 or less tubercles contacts with each other in femur region (4–20 in *G. nebulozonatus* versus 6–37 in *G. kuroiwae*; Fig. 6); single most-enlarged scale on pes base (versus two or more most-enlarged scales; Fig. 7); MS-III absent (versus complete or incomplete); DB-III present (versus absent); and dorsal stripes/bands diffused (versus sharp; Fig. 8). In addition to these diagnostic keys, the new species differs from the Iejima population of *G. kuroiwae* in usually lacking DB-I (versus present) and, if present, DB I is narrow as six or fewer granular scales baring it (4–7 in *G. nebulozonatus* versus 6–10 in *G. kuroiwae*); and often having four or fewer tubercles on the edge of DB-IV (0–8, often four or less in *G. nebulozonatus* versus 3–11, usually five or more in the Iejima *G. kuroiwae*; Fig. 9). The Okinawajima populations of *G. nebulozonatus* is also distinguishable from *G. kuroiwae*, except for the Iejima population, in satisfying more than half of five characters, of which three are the above mentioned MS-III, DB-III, and diffusion of dorsal stripes/bands, and the remaining two are absence or incompleteness of MS-II (versus complete) and presence of DB-II (versus absent). This species differs from *G. yunnu* in showing less posteriorly extended maxillary shelf; lateral inclination of the lateral wall of the posterior part of maxilla; and vertical anterior parts of lateral prefrontal facets of frontal (Nakamura et al., 2014).

FIG. 6. A comparison of femur tubercle conditions between *G. nebulozonatus* (left; KUZ R88884) and *G. kuroiwae* (right; OPM H1502622). Arrows indicate the points of contact between two neighboring tubercles on the dorsal surface of the femur region.

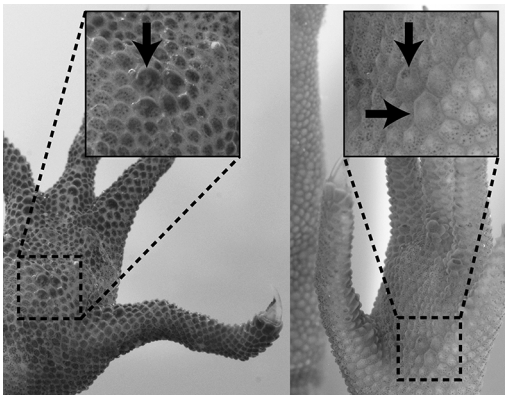

FIG. 7. The most-enlarged scales of pes in *G. nebulozonatus* (left; KUZ R88884) and *G. kuroiwae* (right; OPM H1502622). Arrows in boxes indicate the most-enlarged scales.

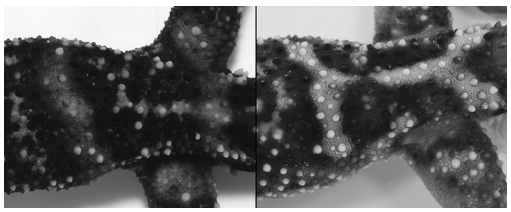

FIG. 8. The sharpness of dorsal stripes/bands on the posterior part of the trunk dorsum in *G. nebulozonatus* (left; KUZ R88884) and *G. kuroiwae* (right; OPM H1502589).

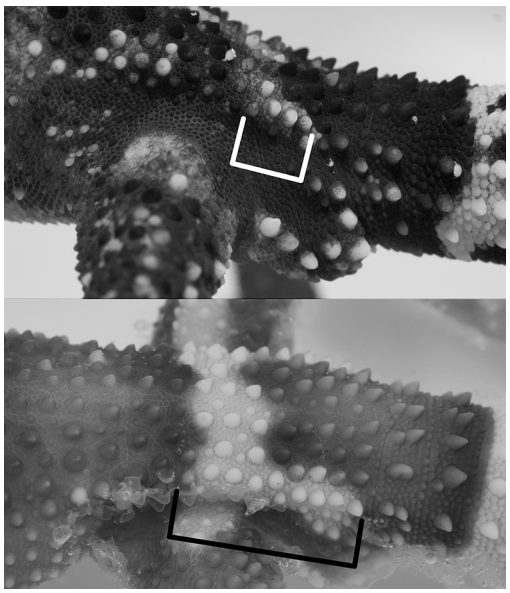

FIG. 9. Anterior–posterior extension of the lateral edges of DB-IV and a series of tubercles on the edge line in *G. nebulozonatus* (top; KUZ R88884) and *G. kuroiwae* (bottom; KUZ R73392).

Description of holotype

An adult male, with the following measurements: snout–vent length 79.8 mm; head length 20.8 mm; head width 14.3 mm; head depth 8.9 mm; snout length 7.6 mm; jaw length 12.4 mm; jaw width 10.4 mm; eye diameter 5.2 mm; interorbital width 2.7 mm; ear opening length 2.6 mm; nape width 8.1 mm; axilla–groin length 37.1 mm; brachial length 10.2 mm; forearm length 13.0 mm; femur length 13.9 mm; crus length 14.3 mm; and tail length 78.1 mm.

Head moderate in size, triangle, distinct from neck in dorsal profile, flat, equal to neck in lateral profile; snout short, acute angle in dorsal view, its tip convex in lateral view; nostril round, opens laterally; eye large, opens laterally, covered with movable eyelid, not seen in ventral view; pupil vertically-elongated without notch; interorbital region narrow; mouth slit deep, its posterior end not exceed posterior edge of eye, followed by shallow dermal lobe not reaching ear opening; ear opens laterally, elongated in dorsoposterior–ventroanterior direction; scales on head granular, weakly raised, juxtaposed, interspaced with conical tubercles posterior to level of ear opening on dorsal, posterior to eye opening on lateral surfaces; rostral trapezium, high as exceeds the level of nostril center, twice as wide as height, slightly concave dorsal edge without notch/groove, bordered by three internasals, supranasals, nasals, and first supralabials; nasal bordered by rostral, supranasal, first supralabial, and seven/eight (left/right) granular or slightly-enlarged flat scales; three post-internasals; 25/26 snout scales including one enlarged scale anterior to eye; 9/12 tubercles on basal edge of eyelid; a row of slightly-enlarged conical scales and a row of slightly-enlarged slightly-raised conical scales on marginal edge of eyelid; 65/65 scales surrounding eye; a spinal tubercle on anterior edge of ear opening; 9/9 supralabials extending to the level of center of eye; 10/10 infralabials exceeding eye center but not reaching posterior edge of eye; mental triangular, wider than height, having round posterior tip exceeding anterior edge of second infralabials, bordered by first infralabials and six postmentals; eight post-postmentals; two to four (increasing in number posteriorly) enlarged flat scale rows along with infralabials; small, slightly-raised, conical, juxtaposed granular scales on ventral side of head; throat scales larger than head-vent scales, round, raised anteriorly, juxtaposed or slightly-imbricate.

Body slender, elongate, slightly-dilated

dorsoventrally; axillary pockets shallow; hemipenal bulges apparent; dorsal to ventrolateral surface of trunk covered by small, smooth, dome-shaped, juxtaposed granular scales almost equal in size, intermixed with enlarged smooth conical tubercles irregularly arranged; dorsal conical tubercles various in size, with large ones bordered by 11–14 (median=12) granular scales, pointed distally on trunk, distal-posteriorly on lumbar and base of tail; 29/29 paravertebral tubercles; 26–28 (median=27) mid-body tubercle rows; 146 granular scales on transverse row of mid-body; 197 ventral scales, slightly-enlarged, slightly-raised, round to oval, slightly-imbricate on thorax to enlarged, flat, imbricate on hind-limb insertions; no precloacal/femoral pores; scales around cloaca small, slightly-raised, oval, slightly-imbricate; 14 postcloacal scales; five/four postcloacal tubercles on edge of hemipenal bulges; a pair of enlarged scales on mid-ventral part of posterior edge of hemipenal bulge.

Forelimbs moderate length, robust; brachium covered with small, well-raised dome-like, juxtaposed or slightly-imbricate granular scales intermixed with enlarged conical tubercles on dorsum, covered with same type of granular scales to dorsal side but fewer tubercles on ventral side; scales of forearms similar to brachium but more dilated and tubercles rarely seen on ventral side; manus scales slightly-raised or flat, juxtaposed, with one/one most-enlarged, raised scale on carpus; one or two strongly-raised hexagonal scales on base of fingers; subdigital scales of fingers less than twice as wide as adjacent rows, raised, trapezoid except for terminal-most triangle scale, juxtaposed or slightly-imbricate; 8-15-17-19-14/9-15-18-17-13 subdigital scales on first to fifth fingers, respectively; hind limbs longer than forelimbs; dorsal to lateral surface of femur and crus covered by well-raised dome-like, juxtaposed or slightly imbricate granular scales larger than those on trunk dorsum, intermixed with slightly to strongly enlarged conical tubercles; tubercles on femur surrounded by 10–14 (median=12) granular scales or other tubercles; some hind-limb tubercles in contact with other tubercles, with 12/16 contact points on femur; femur ventral covered with enlarged, slightly-raised, round, imbricate scales proximally and with those similar to femur-dorsum granular scales distally; ventral scales on crus raised, round, slightly imbricate, aligned to some extent; pes scales slightly-raised, polygonal, juxtaposed to slightly-imbricate, with one/one most-enlarged, raised scale on base; one or two strongly-raised round scales on base of toes; subdigital scales of toes twice or less as wide as adjacent rows, raised, trapezoidal or rectangular except for terminal-most triangle scale, slightly-imbricate; 9-15-20-21-19/8-15-20-23-18 subdigital scales on first to fifth toes, respectively; claws thick, unsheathed, strongly recurved at terminal quarter, bordered by six small scales.

Tail intact, long, segments visible until 14th from the base but not in more distal part; caudal scales arranged in segmented whorls; dorsocaudal scales up to twice as large as dorsal granular scales, raised dorsoposteriorly, round to squared, juxtaposed or slightly-imbricate on caudal base, gradually decreasing in size and height posteriorly; subcaudals enlarged, flat, round to squared, imbricate on base, gradually decreasing in size posteriorly; each caudal segment has 14 (basal segment) to 11 (segment at half of tail) tubercle rows consisting of one or two enlarged tubercles strongly pointed dorsoposteriorly, gradually decreasing in size and height; paravertebral caudal tubercles separated by five to six scales.

In life (Fig. 5), iris reddish brown; ground color of dorsal surface of head, trunk, and limbs dark brown; nuchal loop rudimentary, only present as small tanned-orange blotches above ear openings and short transverse blotch on center of occiput; MS-I complete, pale orange in color, as wide as 6–8 (median=8) granular scales; highly diffused DBs-I–IV present, dark tanned-orange, as wide as 6–8 (median=7), 9–12 (11), 11–12 (11), and 8–13 (10) granular scales, respectively; DB-I extending to forelimb insertion but slightly separated by lateral dark-colored zone; DBs-II

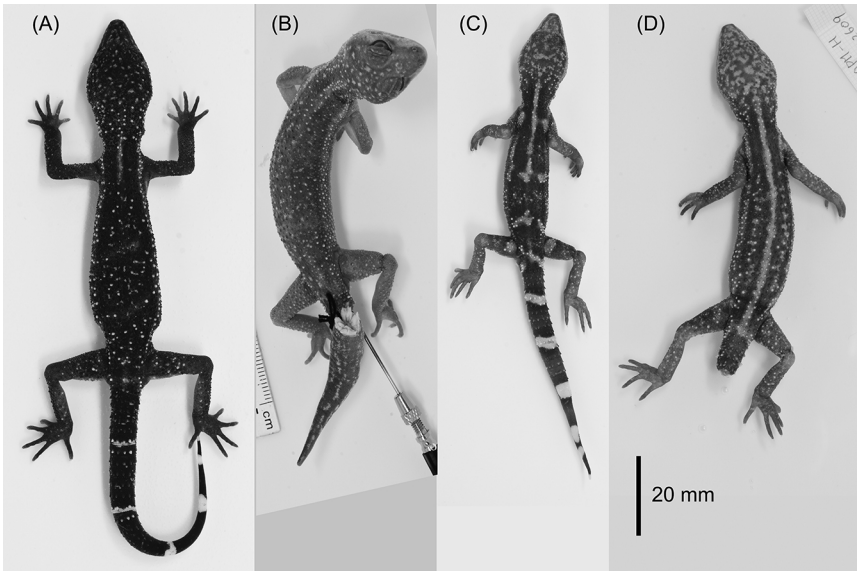

FIG. 10. Paratypes and a non-type specimen of *G. nebulozonatus* with various conditions of dorsal stripe and banding patterns. (A; Benoki) KUZ R88885, with highly diffused dorsal bands; (B; Yona) TPN 77082102, with a completely faded pattern on the dorsum, (C; Yona) OPM H1502607, with sharp dorsal stripe/band edges, and (D; Yona) OPM H1502609, with a complete dorsal stripe and no bands, respectively.

and III obliquely arranged from right to left posteriorly; DB-IV extending to dorsolateral sides of lumbar but not to hind limbs, with a bright-colored tubercle row consisting of four/five tubercles in a linear manner; amorphous, roughly-equal to ear opening but various-sized, light yellow blotches on head dorsum and interspace regions of DBs-II, III, and IV (interspace mottling); light yellow line between supralabials and nostril–eye line; orbital regions including upper eyelids bluish; eyelid fringe orange; faded orange patches on dorsal surface of elbow, proximal part of femur, and knee; pale yellow tubercles on dorsal surface of nape and trunk, lateral line of trunk, ventrolateral sides of trunk, dorsal sides of limbs, and hemipenal bulges; ventral side of head, trunk, and limbs uniformly gray; ground color of tail black; six white (partly interrupted) bands, including tip of tail, encircle tail; saddle-shaped white bands on interspace regions of first to fourth proximal caudal bands on ventral side of tail. In preservation, dark ground color slightly heightened, mid-dorsal stripe, dorsal bands, blotches, limb patches, and bright-colored tubercles turned to gray.

Variation (Fig. 10)

The holotype of *G. nebulozonatus* is characterized within the conspecific individuals examined by several features summarized in Table 2: a relatively small-sized adult male (when compared to other individuals examined that reached a maximum of up to 93.9 mm); upper limits of infralabials (7–10), internasals (1–3), post-internasals (1–3), mid-body tubercle rows (21–27), paravertebral tubercles (24–29), DB-I scales (4–7), DB-II scales (3–11), DB-III scales (5–11), subdigital scales on the fourth fingers (13–19), and subdigital scales on the fourth toe (17–23); MS-IV absent (versus 50.5% individuals incomplete), nuchal loop rudimentary (43.2% absent), DB-I present (81% absent), and DB-I extending to forelimb insertions (71.8% separated). Besides the above characters, a female paratype KUZ R88885 with 90.6 mm in SVL differs in having markedly nebulous mid-dorsal stripe

and dorsal bands with faded dark brown areas, and a tubercle-sized mottling on the head and trunk dorsum (Fig. 10A). Brown granular scales are scattered on the ventral surface of the head. The dorsal pattern can be completely absent as found in a non-type specimen TPN 77082102 (Fig. 10B). A paratype OPM-H 1502607 (Fig. 10C) and two non-type specimens (OPM H1044 and TPN 78042307) have sharp mid-dorsal stripe and dorsal bands. Five paratypes and seven non-type specimens lack DBs-I–III, of which nine also lack DB-IV. However, a paratype OPM H1502609 and two non-type specimens (OPM H1043 and H1502618) have a complete or nearly complete mid-dorsal stripe from the nape to the tail base (Fig. 10D). Size, density, and distribution of mottling on the head and trunk dorsum vary among individuals: scarce mottling less than half of ear-opening in size exists on the head and those on the trunk dorsum mere tubercle-sized in a paratype OPM H1502596, mottling on the head forming network in a paratype OPM H1502605, and no mottling from the nape to the anterior part of the trunk dorsum in a paratype OPM H1502613. Seven of 10 Kourijima individuals (photographic records only) lack DBs-II and III and a sharp stripe/band edge. Many paratypes and non-type specimens have regenerated part of the tail (e.g., TPN 77082102: Fig. 10B), which is thickened, has no segmentation and tubercles, and shows amorphous small bright blotches. Most of juveniles, especially hatchlings, do not have mottling on head and interspace regions of trunk dorsum, and instead, uniformly gray or black, or faded mottling if any. Hemipenal bulges are not swollen in females and juveniles. Intraspecific genetic divergence is known between the Kunigami and Ogimi+ Kourijima areas based on mtDNA (Kurita et al., 2018).

Etymology

The specific epithet *nebulozonatus* is from the Latin nouns “nebula” (figuratively meaning obscurity) and “zona” (band), referring to diffused transverse bands on the trunk dorsum in this species.

Geographic range

The northern part of Okinawajima Island (Kunigami Village, the northern part of Ogimi Village, and probably Higashi Village) and Kourijima Island of Nakijin Village, Okinawa Prefecture, Japan.

Natural history

Goniurosaurus nebulozonatus is a nocturnal and ground-dwelling gecko as other congeners are. It is found in various environments, from sandstone mountains to limestone karst, coastal vegetation areas almost 0 m a.s.l. to mountain forest approximately 400 m a.s.l. covered with primary broad-leaved evergreen forests, as well as in parks, graves, and roadsides with considerable human disturbances. Gravid females are observed from June to early September, and juveniles appear in early September. This species mainly consumes large invertebrates, such as earthworms, spiders, centipedes, crickets, cockroaches, and insect larvae (Kurita and Toda, 2022). The presence of hybrid swarms with *G. kuroiwae* are known from the north-central part of Okinawajima.

Goniurosaurus kuroiwae (Namiye, 1912)
(Japanese name: Kuroiwa Tokage-modoki)

Gymnodactylus albofasciatus kuroiwae: Namiye, 1912
Eublepharis kuroiwae kuroiwae: Nakamura & Uéno, 1963 (in part)
Amamisaurus kuroiwae: Börner, 1981 (in part)
Goniurosaurus kuroiwae: Grismer, 1987 (in part)
Goniurosaurus kuroiwae: Ota, 1989 (in part)
Goniurosaurus kuroiwae kuroiwae: Grismer et al., 1994 (in part)
Goniurosaurus kuroiwae orientalis: Grismer et al., 1994 (Iejima population)
Goniurosaurus kuroiwae kuroiwae: Honda et al., 2014 (as southern Okinawajima population)
Goniurosaurus kuroiwae kuroiwae: Honda and

FIG. 11. The holotype of *Goniurosaurus kuroiwae* (NSMT H2525). Dorsal (top), lateral (middle), and ventral (bottom) views, with collection label information.

Ota, 2017 (as southern Okinawajima population)
Goniurosaurus kuroiwae cf. *kuroiwae*: Honda and Ota, 2017 (Iejima population)
Goniurosaurus kuroiwae: Kurita et al., 2018 (as southern species)

Holotype

NSMT H2525 (Fig. 11), a juvenile, putatively male, collected on September 1909 by Tsune Kuroiwa (also Kou Kuroiwa or formally Hisashi Kuroiwa) from Tano-dake Mountain (locality [11] in Fig. 1), Nago City, Okinawa, Japan (Namiye, 1912).

Other specimens/photographic records examined

See Appendix 2 for examined specimens. In summary, four specimens from Genka–Haneji area, Nago City, one from Motobu Town, two from Sesokojima Island, one from Yomitan Village, one from Uruma City, 67 from Naha City, 60 from Seihua Utaki, Nanjo City, one from Yaese Town, and six from Iejima Island. In addition, the following photographic records were examined: 10 from Genka–Haneji, seven from Yagajijima, seven from Aritsu, Nago, 18 from Ohkawa, Nago, 59 from Motobu, two from Sesokojima, 20 from Ginoza Town, 21 from Yomitan, three from Okinawa–Uruma, 19 from Urasoe–Naha, two from Seihua, 54 from Nanjo–Yaese, three from Itoman City, and 65 from Iejima.

Diagnosis (Table 2)

A moderate-sized *Goniurosaurus* gecko (ca. 75–95 mm SVL for adults; can exceed 100 mm [Tanaka and Nishihira, 1989]). See the diagnosis section of the description of *G. nebulozonatus* for discrimination of *G. kuroiwae* from the other congeners. *Goniurosaurus kuroiwae* differs from *G. nebulozonatus* in satisfying more than half of the following five character status: 6–37 tubercles contacts with each other in the femur region (versus 4–20 in *G. nebulozonatus*); two or more most-enlarged scales on the pes base (versus single most-enlarged scale); MS-III complete or incomplete (versus absent); DB-III absent (versus present); and dorsal stripes/bands sharp (versus diffused). This species and *G. yunnu* have not been directly compared.

Description of holotype

A juvenile, putatively male as judged from slightly swollen hemipenal bulges. The measurements of the holotype are: snout–vent length 50.2 mm; head length 15.0 mm; head width 10.2 mm; head depth 5.9 mm; snout length 5.5 mm; jaw length 9.2 mm; jaw width 8.6 mm; eye diameter 3.9 mm; interorbital width 1.9 mm; ear opening length 1.4 mm (right side); nape width 6.0 mm; axilla–groin length 20.1 mm; brachial length 6.7 mm; forearm length 8.0 mm; femur length 9.9 mm; crus length 10.9 mm; and tail length 49.2 mm.

Head moderate in size, triangle, distinct from neck in dorsal profile, flat, equal to neck in lateral profile; snout short, acute angle in dorsal view, snout tip convex in lateral view;

nostril round, opens laterally; eye large, opens laterally, covered with movable eyelids, not seen in ventral view; pupil difficult to observe; Interorbital region narrow, mouth slit deep, posterior tip not exceed posterior edge of eye, followed by shallow dermal lobe not reaching ear opening; ear opens laterally, elongated in dorsoposterior–ventroanterior direction; scales on head granular, weakly raised, juxtaposed, interspaced with dome-shaped or shallow-conical tubercles posterior to level of ear opening on dorsal, posterior to eye opening on lateral surfaces; rostral rectangle, high as exceeds the level of nostril center, twice as wide as height, slightly concave dorsal edge without notch/groove, bordered by one internasal, supranasals, nasals, and first supralabials; nasal bordered by rostral, supranasal, first supralabial, and eight/nine granular or slightly-enlarged flat scales; one post-internasal; 23/23 snout scales including one enlarged scales anterior to eye; 10/8 tubercles on basal edge of eyelid; a row of slightly-enlarged conical scales and a row of slightly-enlarged slightly-raised conical scales on marginal edge of eyelid; 61/63 scales surrounding eye; a spinal tubercle on anterior edge of ear opening; 9/9 supralabials extending to the level of center of eye; 9/10 infralabials exceeding eye center but not reaching posterior edge of eye; mental triangular, wider than height, has round posterior tip reaching anterior edge of second infralabials, bordered by first infralabials and five postmentals; nine post-postmentals; two to four (increasing in number posteriorly) enlarged flat scale rows along with infralabials; scales on ventral side of head small granular, slightly-raised conical, juxtaposed, interspaced with slightly-enlarged, raised tubercles posterior to level of center of eyes; throat scales larger than head-vent scales, round, raised anteriorly, juxtaposed or slightly-imbricate.

Body slender, elongate, almost cylindrical in section view; no obvious axillary pockets; hemipenal bulges slightly swollen; left side of posterior trunk dissected; small, smooth, dome-shaped granular scales almost equal in size juxtaposed through trunk dorsum–ventrolateral, intermixed with smooth enlarged conical tubercles irregularly arranged; dorsal conical tubercles various in size, with large ones bordered by 11–14 (median=12) granular scales, pointed distally on trunk, distal-posteriorly on lumbar and base of tail; 28/27 paravertebral tubercles; 24 or 25 (median=25) mid-body tubercle rows; 134 granular scales on transverse row of mid-body; ventral scales 195, slightly-enlarged, round to oval, slightly-raised slightly-imbricate on thorax to enlarged, flat, imbricate on hind-limb insertions; no precloacal/femoral pores; scales around cloaca small, oval, raised, slightly-imbricate; 16 postcloacal scales; four/four strongly-raised postcloacal tubercles on edge of hemipenal bulges; a pair of enlarged scales on mid-ventral part of posterior edge of hemipenal bulge.

Forelimbs moderate length, robust; brachium covered with small, raised dome-like, juxtaposed or slightly-imbricate granular scales intermixed with enlarged dome-shaped tubercles on dorsum, ventral side covered with same type of granular scales to dorsal side but fewer tubercles; scales of forearms similar to brachium but more dilated and tubercles rarely seen on ventral side; manus scales raised, juxtaposed, with one/one most-enlarged, raised scale on carpus; one or two strongly-raised hexagonal scales on base of fingers; subdigital scales of fingers less than twice as wide as adjacent rows, raised, trapezoid except for terminal-most triangle scale, juxtaposed or slightly-imbricate; 7-13-14-13-10/8-12-15-15-11 subdigital scales on first to fifth fingers, respectively; hind limbs longer than forelimbs; dorsal to lateral surface of femur and crus covered by granular scales small but larger than those on trunk dorsum, well-raised dome-like, juxtaposed or slightly imbricate, and slightly to strongly enlarged conical tubercles; tubercles on femur surrounded by 10–13 (median=12) granular scales or other tubercles; some hind-limb tubercles in contact with each other, 17/14 contact points on femur; femur ventral covered with enlarged, round, slightly-raised, juxtaposed or slightly-imbricate scales proximally and those similar to femur-dorsum gran-

ular scales distally; ventral scales on crus round, slightly-raised, slightly-imbricate, aligned to some extent; pes scales polygonal, raised, juxtaposed to slightly-imbricate, with one/one most-enlarged, raised scale on base; one or two strongly-raised round scales on base of toes; subdigital scales of toes twice or less as wide as adjacent rows, trapezoidal or rectangular except for terminal-most triangle scale, raised, slightly-imbricate; 8-14-16-17-17/8-12-16-18-15 subdigital scales on first to fifth toes, respectively; claws thick, unsheathed, strongly recurved at terminal quarter, bordered by six or seven (left third finger, left fifth toe, and right fifth toe) small scales.

Tail intact, long, segments visible until 17th from the base but unclear in more distal part; caudal scales arranged in segmented whorls; dorsocaudal scales up to twice as large as dorsal granular scales, raised dorsoposteriorly, round to squared, juxtaposed or slightly-imbricate on caudal base, gradually decreasing in size and height posteriorly; subcaudals enlarged, flat, round to squared, imbricate on base, gradually increasing in size to mid-level of tail length and decreasing in size further posteriorly; each caudal segment has 12 (basal segment) to 10 (segment at half of tail) tubercle rows consisting of one or two enlarged tubercles strongly pointed dorsoposteriorly, gradually decreasing in size and height; paravertebral caudal tubercles on first to fifth basal segments of tail preceded by a smaller tubercle; the biggest tubercles separated by four to six scales.

Color of iris lost in preservation; ground color and pattern of head almost faded; ground color of dorsal surface of trunk, limbs brown; MSs-I and II complete, as wide as six or seven (seven in median) and five or six (six in median) granular scales, respectively; MSs-III and IV absent; nuchal loop may absent, as original description of this species having reported (Namiye, 1912); DBs-I–III absent; a small shoulder patch present on the right side, separated from the base of forelimb insertion, followed by same-sized bright patch on anterior trunk; a short transverse blotch present at the level DB-III; DB-IV present, extending to dorsolateral sides of lumbar, with a bright-colored tubercle row consisting of three/three tubercles in a linear manner, but not to hind limbs; no interspace mottling on trunk dorsum; a faded patch on dorsal surface of proximal part of left femur; no obvious pattern on ventral side of head, trunk, and limbs; ground color of tail brown, slightly-darker than trunk; five white bands encircling tail including tip of tail; diffused, saddle-shaped white bands on interspace regions of first to third proximal caudal bands on ventral side of tail.

Variation (Fig. 12)

The Iejima population differs from the remaining populations of this species especially in dorsal patterns (Table 2); MSs-III and IV absent; obvious occipital patch; DBs-I–IV present and broad; lateral extension of DB-I connecting to forelimb insertion; and a larger number of tubercles on the lateral edge of DB-IV (Fig. 12D and E). However, these features are not fixed within the Iejima population: some individuals possess almost complete mid-dorsal stripes and no transverse bands, which is quite similar to typical Okinawajima individuals.

Most characters of the holotype of *G. kuroiwae* are in the ranges of those of the populations except for Iejima (Table 2). The holotype differs from the majority of Okinawajima specimens in having a single most-enlarged scale on the base of pes (86.9% individuals having two or more most-enlarged scales), lacking MSs-III and IV (48.9% and 66.3% complete, respectively), and having DB-IV (71.3% absent). Among the individuals examined, the presence/absence, size, density, and distribution of mottling on the head and trunk dorsum vary (Fig. 12A–C). Ontogenetic changes of dorsal pattern are slight and fundamental factors of the pattern for each individuals, such as shapes and notches of MSs, do not change with growth (Tokutake et al., 2018).

Etymology

The specific epithet *kuroiwae* is in honor of

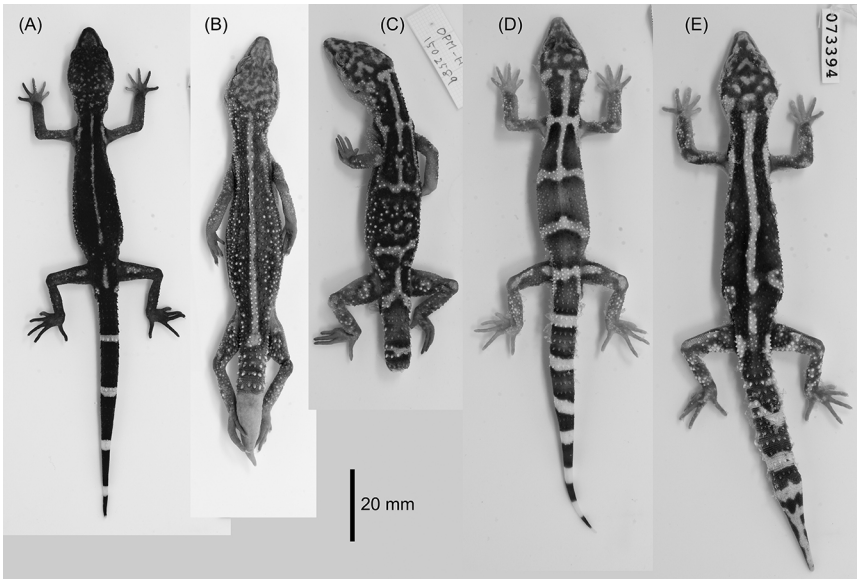

Fig. 12. Variation in the dorsal pattern of *G. kuroiwae*. (A; Tano-dake, Nago) KUZ R88886, a topotype specimen with nearly complete dorsal stripes interrupted in places; (B; Seihua, Nanjo) OPM H1502622 with a complete dorsal stripe; (C; Seihua, Nanjo) OPM H1502589 with the absence of MS-III and the presence of DBs-I and II; (D; Iejima) KUZ R73392 with broad, sharp-edged dorsal bands and MSs-I and II, and (E; Iejima) KUZ R73394 with an almost-complete mid-dorsal stripe but no transverse bands.

the collector of the holotype of this species, Tsune Kuroiwa (1858–1930; formally, Hisashi Kuroiwa; spelled also as Kou Kuroiwa informally), who was the principal of the Kunigami Agricultural School (Namiye, 1912).

Geographic range

The north-central to the southern part of Okinawajima Island (the region south of Nago City and Motobu Peninsula), Yagajijima Island, Sesokojima Island, and Iejima Island, Okinawa Prefecture, Japan.

Discussion

Taxonomic treatment and identification of G. nebulozonatus and G. kuroiwae

Goniurosaurus nebulozonatus, as well as *G. kuroiwae*, encompass wide morphological variation within species, and a glance at the former is sometimes similar to the latter in some aspects and vice versa (Figs. 5 and 9–12). Nevertheless, the random forest modeling and the heat map of the rate of confusion (Fig. 4) indicated that individuals of each species have a certain morphological affinity in total features. An exception is the Iejima population of *G. kuroiwae*, which tended to be confused with *G. nebulozonatus* in the morphological analyses. The Iejima population differs from other conspecific populations in having DB-III (91.5% of examined individuals versus absent in the Okinawajima population [92.8%]) and a larger number of tubercles on the DB-IV edge (3–11 in the Iejima population versus 0–6 in the latter) (Table 2). Despite such morphological differences, the Iejima population is genetically very close to other populations of *G. kuroiwae* in mitochondrial and nuclear DNA markers (Honda et al., 2014; Kurita et al., 2018; this study). These results suggest a rapid morphological divergence in the former population after it was isolated from a part of *G. kuroiwae*, but its reason is unclear at the moment. In this study, the Iejima population was treated as a variation in *G. kuroiwae*, but

TABLE 3. The numbers of correctly and mistakenly identified individuals of *G. nebulozonatus* and *G. kuroiwae* based on the combinations of diagnostic characters at the species level and at the locality level. The numbers in parentheses for populations correspond to Fig. 1. The numbers in brackets indicate the number of diagnostic characters used. Double daggers and asterisks indicate the holotypes of *G. nebulozonatus* (GN) and *G. kuroiwae* (GK), respectively.

		ID scale+pattern [5]		ID scale+pattern [5+3]		ID color pattern only [5]	
		GN	GK	GN	GK	GN	GK
G. nebulozonatus		**33 (0.94)**	**2 (0.06)**	**34 (0.97)**	**1 (0.03)**	**253 (0.93)**	**20 (0.07)**
(1)	Ginama					74 (1.00)	0 (0.00)
(2)	Oku	‡ 1 (1.00)	0 (0.00)	‡ 1 (1.00)	0 (0.00)	‡ 63 (0.98)	1 (0.02)
(3)	Benoki	1 (1.00)	0 (0.00)	1 (1.00)	0 (0.00)	35 (1.00)	0 (0.00)
(4)	Ada					1 (1.00)	0 (0.00)
(5)	Yona	23 (1.00)	0 (0.00)	23 (1.00)	0 (0.00)	43 (0.90)	5 (0.10)
(6)	Aha					2 (1.00)	0 (0.00)
(7)	Hentona-Yonaha	8 (0.80)	2 (0.20)	9 (0.90)	1 (0.10)	15 (0.88)	2 (0.12)
(8)	Kijoka					18 (0.82)	4 (0.18)
(9)	Kourijima					2 (0.20)	8 (0.80)
Hybrid swarm						**30 (0.68)**	**14 (0.32)**
(10)	Tsuha					17 (0.71)	7 (0.29)
(11)	Arume					13 (0.65)	7 (0.35)
***G. kuroiwae* (excl. Iejima)**		**4 (0.03)**	**133 (0.97)**	**12 (0.09)**	**125 (0.91)**	**57 (0.16)**	**305 (0.84)**
(12)	Genka-Haneji	0 (0.00)	* 4 (1.00)	* 3 (0.75)	1 (0.25)	5 (0.36)	* 9 (0.64)
(13)	Yagajijima					1 (0.14)	6 (0.86)
(14)	Aritsu					0 (0.00)	7 (1.00)
(15)	Ohkawa					7 (0.39)	11 (0.61)
(16)	Motobu	0 (0.00)	1 (1.00)	0 (0.00)	1 (1.00)	13 (0.22)	47 (0.78)
(17)	Sesokojima	0 (0.00)	2 (1.00)	0 (0.00)	2 (1.00)	0 (0.00)	4 (1.00)
(18)	Ginoza					10 (0.50)	10 (0.50)
(19)	Yomitan	0 (0.00)	1 (1.00)	0 (0.00)	1 (1.00)	2 (0.09)	20 (0.91)
(20)	Okinawa-Uruma	0 (0.00)	1 (1.00)	0 (0.00)	1 (1.00)	0 (0.00)	4 (1.00)
(21)	Urasoe-Naha	2 (0.03)	65 (0.97)	6 (0.09)	61 (0.91)	13 (0.15)	73 (0.85)
(22)	Seihua	1 (0.02)	59 (0.98)	2 (0.03)	58 (0.97)	3 (0.05)	59 (0.95)
(23)	Nanjo-Itoman	1 (1.00)	0 (0.00)	1 (1.00)	0 (0.00)	3 (0.05)	55 (0.95)
***G. kuroiwae* (Iejima)**		**5 (0.83)**	**1 (0.17)**	**1 (0.17)**	**5 (0.83)**	**50 (0.70)**	**21 (0.30)**
(24)	Iejima	5 (0.83)	1 (0.17)	1 (0.17)	5 (0.83)	50 (0.70)	21 (0.30)

future studies on the evolutionary background of this unique population may require further taxonomic revision.

The species identification based on the majority rule of five scale and dorsal-pattern characteristics (see diagnosis) functioned well with 80%–100% accuracy at the species level (Table 3), except for the geckos from the Iejima population. In this system, five of the six specimens from Iejima were erroneously assigned to *G. nebulozonatus*. However, the identification accuracy was improved to 83% (five out of the six individuals were correctly assigned) when the other three characters were added specifically for the Iejima population.

All *Goniurosaurus* species in the Ryukyus

are endangered and protected, and a substantial number of specimens are only available from a limited number of populations. Therefore, the effective use of non-invasive photographic records was considered. The morphological analyses also provided a diagnosis based only on dorsal-pattern characters to discriminate *G. nebulozonatus* and *G. kuroiwae*. The results suggest that the dorsal pattern characteristics generally functioned well in identifying these species, although the identification accuracy still varies depending on the population (Table 3). Identifications using photo images may enable researchers to conduct field surveys easily, especially for nonprofessional scientists because it is generally not easy for them to get permission to directly handle the animals. Further improvement in species identification accuracy by dorsal patterns is needed to stimulate future studies.

Phylogenetic implications of the Ryukyu Goniurosaurus species

Based on SNP data, the result of the phylogenetic inference for the *Goniurosaurus* spp. in the Okinawa Islands Group is largely congruent with the phylogenetic tree based on mtDNA depicted by Honda et al. (2014). Both studies indicated existences of three groups: (1) *G. toyamai* in Iheyajima, (2) *G. kuroiwae* and *G. nebulozonatus* in Okinawajima and several satellite islands, and (3) *G. orientalis*, *G. yamashinae*, and *G. sengokui* on the southwestern islands (Fig. 2). The relationship among these three groups was unresolved in this study, whereas the unity of *G. kuroiwae* and *G. nebulozonatus* was not well-supported by Honda et al. (2014). The genetic feature of the population of *G. sengokui* from Akajima were examined for the first time in this analysis. This population was considered extinct because of the long absence of a second record after the first discovery in 1981 (Toyama, 1983; Honda and Ota, 2017). Therefore, Honda and Ota (2017) examined a single record (photograph) for this putative population and put it in *G. sengokui*. Afterward, the gecko was rediscovered from the island, and we had a chance to examine them. The adequacy of placing the Akajima population in *G. sengokui* was supported by molecular data in this study (Fig. 2).

Among the phylogeography of amphibians and reptiles in the Okinawa Islands Group, Iheyajima (and a few nearby islands) populations are often diverged first from other populations, e.g., *Hebius pryeri* (Kaito and Toda, 2016), *Sinomicrurus boettgeri* (Kaito et al., 2017), *Microhyla okinavensis* (Tominaga et al., 2019), and *Ateuchosaurus okinavensis* (Makino et al., 2020, 2023), but see the cases of *Plestiodon marginatus* (Kurita and Hikida, 2014) and *Buergeria japonica* (Tominaga et al., 2015). Iheyajima and nearby islands are located on a submarine plateau isolated from the major plateau consisting of most other islands, including Okinawajima. These two plateaus are separated by a sea of >200 m in depth; thus, they may have been isolated from each other for a long time. Remarkable genetic divergences of the Iheyajima (and nearby islands) populations in several species including *G. toyamai* may reflect this geographical feature.

The genetic divergence between the populations in Okinawajima and the southwestern islands is puzzling. The latter is located in the same submarine plateau as the former, and at least Tokashikijima and Akajima (as well as many surrounding islands) have been connected with Okinawajima during the last glacial maxima (Japan Association for Quaternary Research, 1987). Therefore, all amphibians and reptiles on Tokashikijima have conspecific populations in Okinawajima except for *G. sengokui*. Even at the intraspecific level, the Tokashikijima and Akajima populations seldom diverge from populations on Okinawajima, e.g., *Cynops ensicauda* (Tominaga et al., 2010), *Echinotriton andersoni* (Honda et al., 2012), *B. japonica* (Tominaga et al., 2015), *M. okinavensis* (Tominaga et al., 2019), *H. pryeri* (Kaito and Toda, 2016), *S. boettgeri* (Kaito et al., 2017), and *A. okinavensis* (Makino et al., 2020), but see the case of *Babina holsti* (Tominaga et al., 2014). The large genetic dif-

ferentiation between these two regions in *Goniurosaurus* is open to question. Kurita et al. (2018) argued that the deeper genetic divergence among allopatric populations in *Goniurosaurus* geckos might be caused by more frequent retention of previously diverged local lineages when population size had shrunk in the geohistorical time scale. This study detected a certain degree of genetic divergence even between Akajima and Tokashikijima, although the two islands are only 5 km away from each other in a shallow sea. Despite the possible contact of *Goniurosaurus* populations there during the last glacial maxima, they have somewhat retained their genetic features. This argument might be highly related to why *G. kuroiwae* and *G. nebulozonatus* do not fuse genetically. Also, it cannot be explained at the moment how and where these two species in Okinawajima emerged. More extensive genomic analyses of detailed population histories may answer these questions.

Acknowledgments

We thank to S. Tanaka for allowing us access to preserved specimens (TPN series and those donated to OPM), J. Yamazaki and A. Kikukawa for helping us loan the specimens deposited in the OPM, N. Yoshikawa for allowing us to examine the holotype of *G. kuroiwae*, and T. Hikida for the loan of specimens in the KUZ. We also thank T. Hikida and H. Nagamasu for the critical advice about nomenclature. We appreciate H. Takahashi for the information of the Akajima population of *G. sengokui*. The first author deeply thanks R. Kawamura for great assistance in field surveys. We are grateful for anonymous reviewers for critical comments helping us to revise the manuscript. This research was performed by the Environment Research and Technology Development Fund (JPMEERF20204002) of the Environmental Restoration and Conservation Agency of Japan. It was also partially supported by grants from the Japan Society for the Promotion of Science (JSPS KAKENHI Grant Nos. 22510244 and 22570094), the Pro Natura Fund (in 2018), and the Zoshinkai Fund for Protection of Endangered Animals (in 2012 and 2018). All *Goniurosaurus* species in the Ryukyus are strictly protected by laws and ordinances, and this study was conducted with the permission from the Ministry of the Environment of Japan, the Kagoshima Prefectural Board of Education, and the Okinawa Prefectural Board of Education. Computations were partially performed on the NIG supercomputer at ROIS National Institute of Genetics. The authors would like to thank Enago (www.enago.com) for the English language review.

Data Availability

Supplementary materials are available at figshare: https://doi.org/10.6084/m9.figshare.24911478

Literature Cited

Alexander, D. H., Novembre, J., and Lange, K. 2009. Fast model-based estimation of ancestry in unrelated individuals. *Genome Research* 19: 1655–1664.

Andrews, S. 2010. FastQC: a quality control tool for high throughput sequence data. Available via http://www.bioinformatics.babraham.ac.uk/projects/fastqc/

Barbour, T. 1908. Some new reptiles and amphibians. *Bulletin of the Museum of Comparative Zoology at Harvard College* 51: 315–325.

Börner, A. R. 1981. The genera of Asian eublepharine geckos and a hypothesis of their phylogeny. *Miscellaneous Articles in Saurology* 9: 1–14.

Catchen, J., Hohenlohe, P., Bassham, S., Amores, A., and Cresko, W. 2013. Stacks: an analysis tool set for population genomics. *Molecular Ecology* 22: 3124–3140.

Chang, C. C., Chow, C. C., Tellier, L. C. A. M., Vattikuti, S., Purcell, S. M., and Lee, J. J. 2015. Second-generation PLINK: rising to the challenge of larger and richer datasets. *GigaScience* 4: s13742-015-0047-8.

Chen, S., Zhou, Y., Chen, Y., and Gu, J. 2018. fastp: an ultra-fast all-in-one FASTQ preproces-

sor. *Bioinformatics* 34: i884–i890.

Grismer, L. L. 1987. Evidence for the resurrection of *Goniurosaurus* Barbour (Reptilia: Eublepharidae) with a discussion on geographic variation in *Goniurosaurus lichtenfelderi*. *Acta Herpetologica Sinica* 6: 43–47.

Grismer, L. L., Ota, H., and Tanaka, S. 1994. Phylogeny, classification, and biogeography of *Goniurosaurus kuroiwae* (Squamata: Eublepharidae) from the Ryukyu Archipelago, Japan, with description of a new subspecies. *Zoological Science* 11: 319–335.

Grismer, L. L., Viets, B. E., and Boyle, L. J. 1999. Two new continental species of *Goniurosaurus* (Squamata: Eublepharidae) with a phylogeny and evolutionary classification of the genus. *Journal of Herpetology* 33: 382–393.

Guindon, S., Dufayard, J.-F., Lefort, V., Anisimova, M., Hordijk, W., and Gascuel, O. 2010. New algorithms and methods to estimate maximum-likelihood phylogenies: assessing the performance of PhyML 3.0. *Systematic Biology* 59: 307–321.

Hoang, D. T., Chernomor, O., von Haeseler, A., Minh, B. Q., and Vinh, L. S. 2018. UFBoot2: improving the ultrafast bootstrap approximation. *Molecular Biology and Evolution* 35: 518–522.

Honda, M. 2002. Conservation genetics of *Goniurosaurus kuroiwae kuroiwae*, with special reference to a population from the central part of Okinawajima Island, Ryukyu Archipelago. *Akamata* (16): 15–18.

Honda, M., Kurita, T., Toda, M., and Ota, H. 2014. Phylogenetic relationships, genetic divergence, historical biogeography and conservation of an eublepharid gecko, *Goniurosaurus kuroiwae* (Squamata: Eublepharidae), from the Central Ryukyus, Japan. *Zoological Science* 31: 309–320.

Honda, M., Matsui, M., Tominaga, A., Ota, H., and Tanaka, S. 2012. Phylogeny and biogeography of the Anderson's crocodile newt, *Echinotriton andersoni* (Amphibia: Caudata), as revealed by mitochondrial DNA sequences. *Molecular Phylogenetics and Evolution* 65: 642–653.

Honda, M. and Ota, H. 2017. On the live coloration and partial mitochondrial DNA sequences in the topotypic population of *Goniurosaurus kuroiwae orientalis* (Squamata: Eublepharidae), with description of a new subspecies from Tokashikijima Island, Ryukyu Archipelago, Japan. *Asian Herpetological Research* 8: 96–107.

Hosoya, S., Hirase, S., Kikuchi, K., Nanjo, K., Nakamura, Y., Kohno, H., and Sano, M. 2019. Random PCR-based genotyping by sequencing technology GRAS-Di (genotyping by random amplicon sequencing, direct) reveals genetic structure of mangrove fishes. *Molecular Ecology Resources* 19: 1153–1163.

Huson, D. H. and Bryant, D. 2006. Application of phylogenetic networks in evolutionary studies. *Molecular Biology and Evolution* 23: 254–267.

Japan Association for Quaternary Research. 1987. *Quaternary Maps of Japan*. University of Tokyo Press, Tokyo.

Kaito, T., Ota, H., and Toda, M. 2017. The evolutionary history and taxonomic reevaluation of the Japanese coral snake, *Sinomicrurus japonicus* (Serpentes, Elapidae), endemic to the Ryukyu Archipelago, Japan, by use of molecular and morphological analyses. *Journal of Zoological Systematics and Evolutionary Research* 55: 156–166.

Kaito, T. and Toda, M. 2016. The biogeographical history of Asian keelback snakes of the genus *Hebius* (Squamata: Colubridae: Natricinae) in the Ryukyu Archipelago, Japan. *Biological Journal of the Linnean Society* 118: 187–199.

Kuhn, M. 2008. Building predictive models in R using the caret package. *Journal of Statistical Software* 28: 1–26.

Kurita, K. and Hikida, T. 2014. Divergence and long-distance overseas dispersals of island populations of the Ryukyu five-lined skink, *Plestiodon marginatus* (Scincidae: Squamata), in the Ryukyu Archipelago, Japan, as revealed by mitochondrial DNA phylogeography. *Zoological Science* 31: 187–194.

Kurita, T., Honda, M., and Toda, M. 2018. Species delimitation and biogeography of the Ryukyu ground geckos, *Goniurosaurus kuroiwae* ssp. (Squamata: Eublepharidae), by use of mitochondrial and nuclear DNA analyses. *Journal of Zoological Systematics and Evolutionary Research* 56: 209–222.

Kurita, T. and Toda, M. 2022. Comparison of

morphological identification and DNA metabarcoding for dietary analysis of faeces from a subtropical lizard. *Wildlife Research* 50: 224–236.

Kursa, M. B. and Rudnicki, W. R. 2010. Feature selection with the Boruta package. *Journal of Statistical Software* 36: 1–13.

Liaw, A. and Wiener, M. 2002. Classification and regression by randomForest. *R News* 2: 18–22.

Maki, M. 1931. A new banded gecko, *Eublepharis orientalis*, sp. nov. from Riu Kyu. *Annotaiones Zoologicae Japonenses* 13: 9–11.

Makino, T., Nakano, T., Okamoto, T., and Hikida, T. 2023. Taxonomic revision and redescription of *Ateuchosaurus pellopleurus* (Hallowell, 1861) (Reptilia, Squamata, Scincidae) with resurrection of *A. okinavensis* (Thompson, 1912). *Zoosystematics and Evolution* 99: 77–91.

Makino, T., Okamoto, T., Kurita, K., Nakano, T., and Hikida, T. 2020. Origin and intraspecific diversification of the scincid lizard *Ateuchosaurus pellopleurus* with implications for historical island biogeography of the Central Ryukyus of Japan. *Zoologischer Anzeiger* 288: 1–10.

Minh, B. Q., Lanfear, R., Trifinopoulos, N. L.-T. J., Schrempf, D., and Schmidt, H. A. 2022. IQ-TREE version 2.2.0: tutorials and manual phylogenomic software by maximum likelihood. Available via http://www.iqtree.org/

Nakamura, Y., Takahashi, A., and Ota, H. 2014. A new, recently extinct subspecies of the Kuroiwa's leopard gecko, *Goniurosaurus kuroiwae* (Squamata: Eublepharidae), from Yoronjima Island of the Ryukyu Archipelago, Japan. *Acta Herpetologica* 9: 61–73.

Nakamura, K. and Uéno, I. 1959. The geckos found in the limestone caves of the Ryu-Kyu Islands. *Memoirs of the College of Science, University of Kyoto* 26: 45–52.

Nakamura, K. and Uéno, S. 1963. *Genshoku Nihon Ryosei Hachurui Zukan [Japanese Reptiles and Amphibians in Colour]*. Hoikusha, Osaka.

Namiye, M. 1912. The geckos from the Okinawa Islands. *Dobutsugaku Zasshi (Zoological Magazine)* 24: 442–445. (in Japanese)

Nguyen, L.-T., Schmidt, H. A., von Haeseler, A., and Minh, B. Q. 2015. IQ-TREE: a fast and effective stochastic algorithm for estimating maximum likelihood phylogenies. *Molecular Biology and Evolution* 32: 268–274.

Okada, Y. 1936. A new cave-gecko, *Gymnodactylus yamashinae* from Kumejima, Okinawa group. *Proceedings of the Imperial Academy of Japan* 12: 53–54.

Ota, H. 1989. A review of the geckos (Lacertilia: Reptilia) of the Ryukyu Archipelago and Taiwan. p. 222–261. *In*: M. Matsui, T. Hikida, and R. C. Goris (eds.), *Current Herpetology in East Asia*. Herpetological Society of Japan, Kyoto.

Ota, H., Honda, M., Kobayashi, M., Sengoku, S., and Hikida, T. 1999. Phylogenetic relationships of eublepharid geckos (Reptilia: Squamata): a molecular approach. *Zoological Science* 16: 659–666.

R Core Team. 2022. R: a language and environment for statistical computing. Available via https://www.R-project.org/

Tanaka, S. and Nishihira, M. 1989. Growth and reproduction of the gekkonid lizard *Eublepharis kuroiwae kuroiwae*. p. 349–357. *In*: M. Matsui, T. Hikida, and R. C. Goris (eds.), *Current Herpetology in East Asia*. Herpetological Society of Japan, Kyoto.

Tokutake, K., Yamazaki, K., and Oka, S. 2018. Individual identification for wild Kuroiwa's ground gecko, *Goniurosaurus kuroiwae kuroiwae*, on the basis of the natural marks. *Bulletin of the Herpetological Society of Japan* 2018: 48–51.

Tominaga, A., Matsui, M., Eto, K., and Ota, H. 2015. Phylogeny and differentiation of wide-ranging Ryukyu Kajika frog *Buergeria japonica* (Amphibia: Rhacophoridae): geographic genetic pattern not simply explained by vicariance through strait formation. *Zoological Science* 32: 240–247.

Tominaga, A., Matsui, M., and Nakata, K. 2014. Genetic diversity and differentiation of the Ryukyu endemic frog *Babina holsti* as revealed by mitochondrial DNA. *Zoological Science* 31: 64–70.

Tominaga, A., Matsui, M., Shimoji, N., Khonsue, W., Wu, C.-S., Toda, M., Eto, K., Nishikawa, K., and Ota, H. 2019. Relict distribution of

Microhyla (Amphibia: Microhylidae) in the Ryukyu Archipelago: high diversity in East Asia maintained by insularization. *Zoologica Scripta* 48: 440–453.

Tominaga, A., Ota, H., and Matsui, M. 2010. Phylogeny and phylogeography of the sword-tailed newt, *Cynops ensicauda* (Amphibia: Caudata), as revealed by nucleotide sequences of mitochondrial DNA. *Molecular Phylogenetics and Evolution* 54: 910–921.

Toyama, M. 1983. Preliminary reports on the herpetological fauna of the Okinawa islands, Ryukyu Archipelago (II). p. 16–22. *In*: Okinawa Prefectural Museum (ed.), *Report of the Okinawa Prefectural Museum III—Zamami-Mura Village*. Okinawa Prefectural Museum, Naha.

Zhu, X. Y., Liu, Y. J., Bai, Y., Román-Palacios, C., Li, Z., and He, Z. Q. 2021. *Goniurosaurus chengzheng* sp. nov., a new species of Leopard Gecko from Guangxi, China (Squamata: Eublepharidae). *Zootaxa* 4996: 555–568.

Accepted: 27 November 2023